# Copyright Warning & Restrictions

The copyright law of the United States (Title 17, United States Code) governs the making of photocopies or other reproductions of copyrighted material.

Under certain conditions specified in the law, libraries and archives are authorized to furnish a photocopy or other reproduction. One of these specified conditions is that the photocopy or reproduction is not to be "used for any purpose other than private study, scholarship, or research." If a, user makes a request for, or later uses, a photocopy or reproduction for purposes in excess of "fair use" that user may be liable for copyright infringement,

This institution reserves the right to refuse to accept a copying order if, in its judgment, fulfillment of the order would involve violation of copyright law.

Please Note: The author retains the copyright while the New Jersey Institute of Technology reserves the right to distribute this thesis or dissertation

Printing note: If you do not wish to print this page, then select "Pages from: first page # to: last page #" on the print dialog screen

NJIT New Jersey's Science & Technology University

The Van Houten library has removed some of the personal information and all signatures from the approval page and biographical sketches of theses and dissertations in order to protect the identity of NJIT graduates and faculty.

## ABSTRACT

### AUTONOMIC NERVOUS SYSTEM EVALUATION USING TIME-FREQUENCY ANALYSIS

by
**Sanjay Fernando**

Spectral analysis of heart rate variability (HRV) provided an estimate of the sympathetic and parasympathetic influences on heart rate without drugs or other invasive procedures. However, there are many situations where heart rate changed rapidly over time and the control of those changes was of considerable interest. Time-frequency analysis was utilized to expand the concept of spectral analysis of HRV to describe changes in vagal tone and sympatho-vagal balance as a function of time. As a result the assessment of the autonomic nervous system during rapid changes in heart rate was made.

There were three advantages to calculating vagal tone and sympatho-vagal balance by using time-frequency analysis. First, vagal tone and sympatho-vagal balance were described as functions of time. Hence, a better understanding was attained about autonomic control of rapidly changing signals. Second, the rate of increase or decrease of vagal tone and sympatho-vagal balance was derived. These rates were used to determine the integrity of the autonomic system. Third, a mental component affecting vagal tone was suggested. It is anticipated that the effects of anxiety on vagal tone can be revealed using time-frequency analysis.

# AUTONOMIC NERVOUS SYSTEM EVALUATION USING TIME-FREQUENCY ANALYSIS

by
Sanjay Fernando

A Thesis
Submitted to the Faculty of
New Jersey Institute of Technology
in Partial Fulfillment of the Requirements for the Degree of
Master of Science in Biomedical Engineering

Biomedical Engineering Committee

October 1994

## APPROVAL PAGE

## AUTONOMIC NERVOUS SYSTEM EVALUATION USING TIME-FREQUENCY ANALYSIS

**Sanjay Fernando**

Dr. Stanley S. Reisman, Thesis Advisor — Date
Professor of Electrical Engineering and Associate
Chairperson for Graduate Studies, NJIT

Dr. David Kristol, Committee Member — Date
Professor of Chemistry and Director of
Biomedical Engineering Program, NJIT

Dr. Thomas W. Findley, Committee Member — Date
Associate Professor of Medicine, UMDNJ
Director of Research, Kessler Institute for
Rehabilitation

## BIOGRAPHICAL SKETCH

**Author:** Sanjay Kanchan Fernando

**Degree:** Master of Science in Biomedical Engineering

**Date:** October 1994

**Undergraduate and Graduate Education:**

- Master of Science in Biomedical Engineering
  New Jersey Institute of Technology, Newark, NJ, 1994

- Bachelor of Science in Electrical Engineering
  New Jersey Institute of Technology, Newark, NJ 1993

**Major:** Biomedical Engineering

**Presentations and Publications:**

Fernando,Sanjay K. Reisman,S., "Autonomic Nervous System Evaluation Using Time-Frequency Analysis." IEEE-SP International Symposium on Time-Frequency and Time-Scale Analysis. Philadelphia, Pennsylvania, October 25-28, 1994.

Fernando,Sanjay K., Reisman,S., Daum,M., Zorowitz,R., DeMeersman,R. "Baroreceptor Reflex Sensitivity Among Stroke Survivors: A Pilot Study." 20th Annual Northeast Bioengineering Conference. Springfield,Massachusetts, March 17 & 18, 1994.

This thesis is dedicated to my parents,
Jayantha and Lakshman Fernando.

## ACKNOWLEDGMENT

The author wishes to express his sincere gratitude to his advisor, Dr. Stanley S. Reisman, for his guidance, friendship and moral support throughout this research.

Special thanks to Dr. David Kristol and Dr. Thomas W. Findley for serving as members of the committee.

The author appreciates the help and suggestions from Dr. Ronald DeMeersman.

## TABLE OF CONTENTS

## TABLE OF CONTENTS
## (Continued)

## LIST OF TABLES

## LIST OF FIGURES

## LIST OF FIGURES
**(continued)**

# CHAPTER 1

# INTRODUCTION

Biomedical engineering is the application of scientific and mathematical principles to medical science. The goal of a biomedical engineer is to develop tools for enhanced diagnosis and treatment of ailments that afflict mankind. The following document chronicles the research conducted on the utilization of time-frequency analysis as a non-invasive tool to quantify rapidly changing biological signals.

## 1.1 Time-Frequency Analysis

Time-frequency analysis was used to describe and understand how the frequency content of a non-stationary signal was changing in time[1]. Traditional analysis dealt with time and frequency analysis separately. Such individual descriptions were good enough for situations where the frequency content was not changing in time. For non-stationary signals traditional analysis does not fully describe what was happening.

For example, the Fourier transform displays the frequencies that existed for the total duration of the signal, not the frequencies which existed at a particular time. By examining the spectrum we can not ascertain when those frequencies existed. The best way to appreciate the need for a combined time-frequency description was by way of a pictorial example. The methods of calculation will be discussed later. Figure 1.1 is the time-frequency distribution of a whale sound. The time wave form was on the left running up the page. The energy density spectrum is shown below the

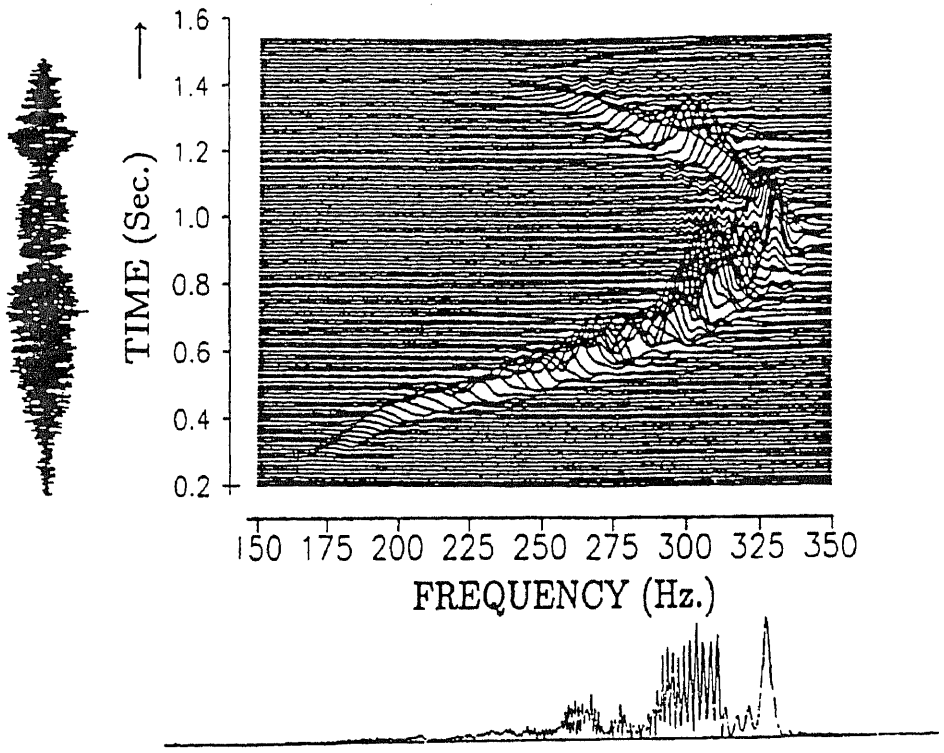


**Figure 1.1** Main square figure is the time-frequency distribution of whale sound. The time wave form is on the left running up the page. The Fourier transform is shown below the main figure. (From Amin,M. et al. "Methods and Applications for Time-frequency Analysis," Conference Notes, University of Michigan,1993)

main figure. An inspection of the time wave form does not yield very much insight, although in principle a great deal of information is present. The power spectrum of the signal appears below the main figure. It shows that the frequencies ranged from 175 to 325 Hz and the magnitude shows the relative strength of each frequency. However, the spectrum represents only the frequencies which existed during the production of the sound; it does not show when they existed. The combined time-frequency picture plots time versus frequency; it shows the frequencies that existed at each time. The time-frequency representation shows the frequency components of the

signal , how long the components lasted and how each component changed in time. From the spectrum nothing can be said about the duration of these components and where in time they existed.

In certain disciplines density functions are called distributions because they indicate how things are distributed. Hence, what is called a density function in mathematics is often called a distribution function in other disciplines. (Unfortunately the term "distribution" in mathematics means something else, namely, the probability of finding the value of the random variable to be less than a certain fixed value.) Physics typically uses the phrase distribution to denote density and since the type of time-frequency density functions considered were first developed in physics the term distribution has stuck; hence the term "time-frequency distribution."

Time and frequency descriptions allowed us to calculate time and frequency

$$<g(\omega)> = \int g(\omega)\,|S(\omega)|^2 d\omega \qquad (1)$$

averages only, that is[2]

$$<g(t)> = \int g(t)\,|s(t)|^2 dt \qquad (2)$$

where $<g(\omega)>$ is the average frequency density and $<g(t)>$ is the average time density. The calculation of average density as a functions of time and frequency was not addressed.

$$<g(t,\omega)>=???$$

Where $<g(t,\omega)>$ is the average density as a function of time and frequency. If we do have a time-frequency description as represented by the combined density $P(t,\omega)$ then we could calculate joint averages of time and frequency by the way of

$$<g(t,\omega)>=\int\int g(t,\omega)P(t,\omega)dtd\omega \tag{3}$$

The short-time Fourier transform was the first tool devised for analyzing a signal in time and frequency[3]. The equation of the distribution is :

$$S_t(\omega)=\frac{1}{\sqrt{2\pi}}\int_{t-\Delta}^{t+\Delta}s(t')e^{-j\omega t'}dt' \tag{4}$$

where s(t') is the time signal and $S_t(\omega)$ is the Fourier transform of a small piece of the signal (figure 1.2). For each different time we selected a corresponding small piece centered around the time,t, which gave a spectrum. The totality of these spectra gave a time-frequency distribution. The selection of the small piece around the time of interest was chosen using a window function. The phrase "window" indicated that we were looking at only certain parts of the signal. We multiplied the signal $s(\tau)$ by the window function, $h(\tau)$, centered around the time of interest $\tau$-t to obtain the weighted signal where $\tau$ was the time centered around the fixed time t (equation 5).

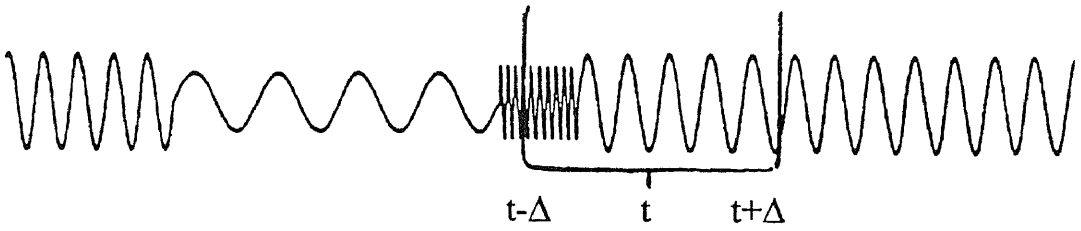


**Figure 1.2** The spectrum of a small piece of the signal around time,t, will emphasize the frequencies at that time. Since the time interval is short compared to the whole signal this process is called short-time Fourier transform. (From Amin,M et al. "Methods and Applications for Time-frequency Analysis" Conference Notes, University of Michigan, 1993)

$$s_h(\tau)=s(\tau)h(\tau-t) \tag{5}$$

Considering this signal as a function of $\tau$ ,we computed its spectrum. Since we presumably have chosen a window that emphasized the time t, the spectrum would emphasize the frequencies at that time. In particular the spectrum was

$$S_t(\omega)=\frac{1}{\sqrt{2\pi}}\int e^{-j\omega\tau}s_h(\tau)d\tau \tag{6}$$

which was the short-time Fourier transform.

The main shortcoming of the short-time Fourier transform was the trade off between time and frequency resolution[2]. In order to improve time resolution we had to choose a window which was very narrow around the point of interest, but that resulted in a modified signal which was also narrow. We had artificially made a short duration signal for the purpose of analysis that created a wide spectrum[4]. This was a consequence of the time-bandwidth relation (uncertainty principle). A narrow window

distorted the original spectrum and introduced a wide spectrum. Hence, good time resolution was achieved with a decreased frequency resolution.

The concept of the short-time Fourier transform was limited by time-frequency resolution. However, resolution limitation may be overcome by using the Wigner distribution[2]. The Wigner distribution (WD) was introduced by Wigner (1932) and incorporated into signal analysis by Ville (1948). The WD maps a one-dimensional function of time into a two-dimensional function of time and frequency (figure 1.3). The WD has served as a useful analysis tool in fields as diverse as quantum mechanics, optics, acoustics, bioengineering, image processing, and oceanography [3]. It has been successfully implemented for the analysis of several biological signals: ECG, [5] blood pressure, respiratory and beat-to-beat fluctuations, attributed to

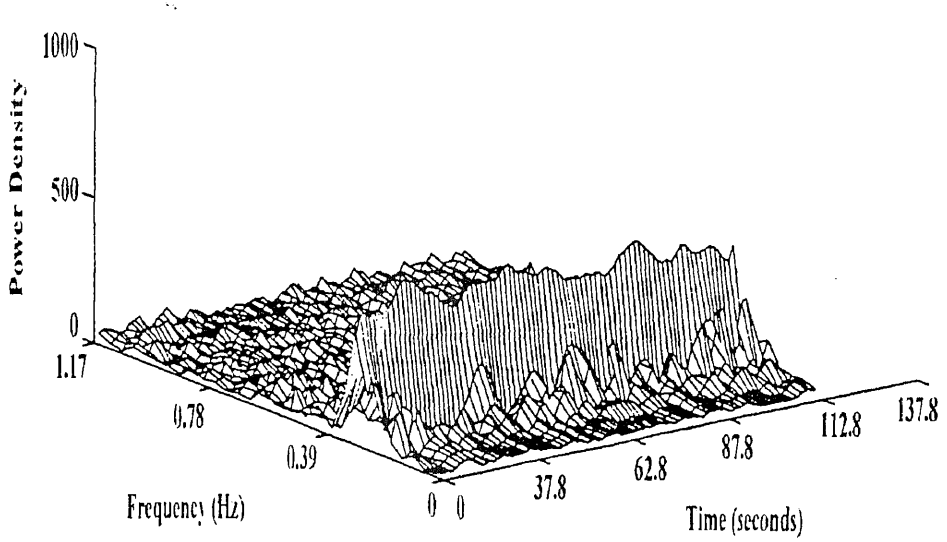


**Figure 1.3** Time-frequency representation

changes in autonomic nervous system activity [6].

The Wigner distribution features perfect time-frequency resolution and also some very interesting mathematical properties [2]. The equation for this distribution is :

$$P_w(t,f)=\int_{-\infty}^{\infty} e^{-j2\pi f\tau} s^*(t-\frac{1}{2}\tau)s(t+\frac{1}{2}\tau)d\tau \qquad (7)$$

where $s(t)=A(t)e^{j\varphi(t)}$ represents the original time signal. A(t) is called the envelope or amplitude; $\varphi(t)$ is the phase. The time around the fixed time t is denoted as $\tau$ . The calculation is performed follows. At the time of interest multiply a piece of the signal to the left with a piece on the right ( or fold the signal about time t ) and repeat it for each $\tau$. That defines $s^*(t-{}^1/_2\tau)s(t+{}^1/_2\tau)$ as a function of $\tau$. Take the Fourier transform with respect to $\tau$. That yields the spectrum for time t. The process is repeated for all times of interest.

The WD satisfies a large number of desirable mathematical properties. There are eleven desirable properties for any time-frequency distribution[7] :

1. "Non negativity"

   A density represents a fraction of the components within a certain range; therefore, it should not be negative.

2. "Realness"

   The density should be real.

3. "Time shift"

   When the original signal is translated by a specific time, the whole distribution

should also be translated by that time.

4. "Frequency shift"

When the original signal is translated by a specific frequency, the whole distribution should be shifted by the same frequency.

5. "Time Marginal"

The individual time density should be satisfied.

$$\int P(t,\omega)d\omega = P_1(t) = |s(t)|^2 \tag{8}$$

where $P_1(t)$ is the time marginal (instantaneous signal power).

6. "Frequency Marginal"

The individual frequency density should be satisfied.

$$\int P(t,\omega)dt = P_2(\omega) = |S(\omega)|^2 \tag{9}$$

where $P_2(\omega)$ is the frequency marginal (signal's power density spectrum).

7. "Instantaneous frequency"

The first-order moment of the $P(t,\omega)$ with respect to $\omega$ gave the instantaneous frequency $\omega(t)$.

$$\omega(t)=\int_{-\infty}^{\infty}\omega * P(t,\omega)d\omega \tag{10}$$

8. "Group delay"

The first-order moment of the P(t,ω) with respect to t gave the group delay τ(ω).

$$\tau(\omega)=\int_{-\infty}^{\infty}t * P(t,\omega)dt \tag{11}$$

9. "Time support"

Signals are finite and therefore have a definite beginning before which they were zero and a definite ending after which they were zero. The time -frequency distribution should be zero before and after the signal and at any other place where the signal was zero.

10. "Frequency support"

Frequency support was comparable to time support. If the signal was bandlimited, the time-frequency distribution would be zero outside the frequency band.

11. "Reduced Interference"

The distribution should not contain cross terms between frequency components. For a multicomponent signal, the spectrum of each signal should

be clearly seen without interference.

The WD satisfies all but two of the desired properties. One undesirable property of the WD is that it is not always positive, property 1. The WD also does not satisfy property 11. If the input signal consists of groups of signals with distinct characteristics, for example

$$\text{if } s(t) = s_o(t) + s_n(t),$$

then its WD can be expressed in terms of its components:

$$W_{s_o+s_n}(t,\omega) = W_{s_o}(t,\omega) + W_{s_n}(t,\omega) + W_{s_o s_n}(t,\omega) \tag{12}$$

where

$$W_{s_o s_n} = \int_{-\infty}^{\infty} e^{-j2\pi f\tau}[s_o(t+\frac{\tau}{2})s_n^*(t-\frac{\tau}{2}) + s_o^*(t-\frac{\tau}{2})S_n(t+\frac{\tau}{2})]d\tau \tag{13}$$

is the WD of the cross terms of $s_o(t)$ and $s_n(t)$ which would cause an additional cross spectrum in the time-frequency representation. For example, figure 1.4 shows the Wigner distribution of a signal composed of the sum of two infinite duration sine waves. The oscillating term in the middle of the two frequencies is the cross term.

In nature signals are real and the spectrum of a real signal satisfies $S(-\omega) = S^*(\omega)$. Therefore the energy density spectrum $|S(\omega)|^2$ was always symmetric about the origin (figure 1.5), that is $|S(\omega)|^2 = |S(-\omega)|^2$. The average frequency would

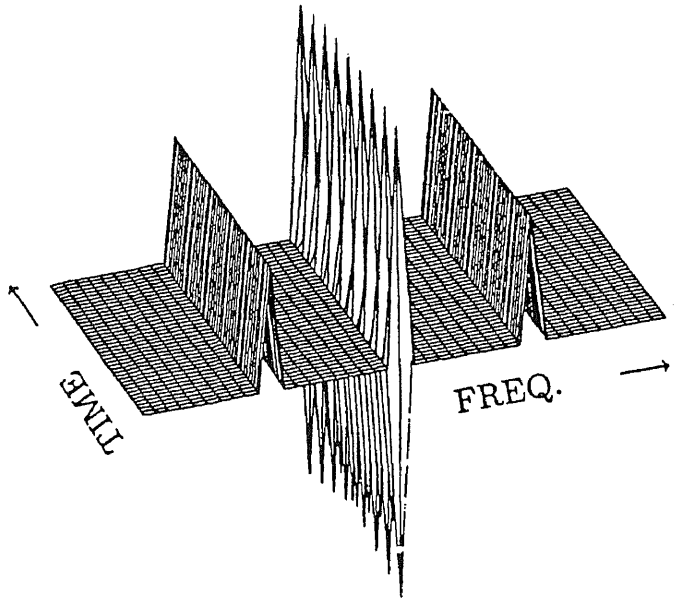


**Figure 1.4** The Wigner distribution of the sum of two infinite duration sine waves. The oscillating term in the middle of the two frequencies is the cross term. (From Amin, M. et al. "Methods and Applications for Time -frequency Analysis" Conference Notes, University of Michigan 1993)

always come out to be zero because of the symmetry and therefore, this did not tells us what was really going on. Secondly, if we wanted the spread of frequencies, the spread would turn out to be roughly the distance between the two peaks while the answer we want was the spread of the individual peaks. To obtain a value for average frequency which was centered in the middle of the right hand peak we must neglect the left peak in the averaging (equation 14).

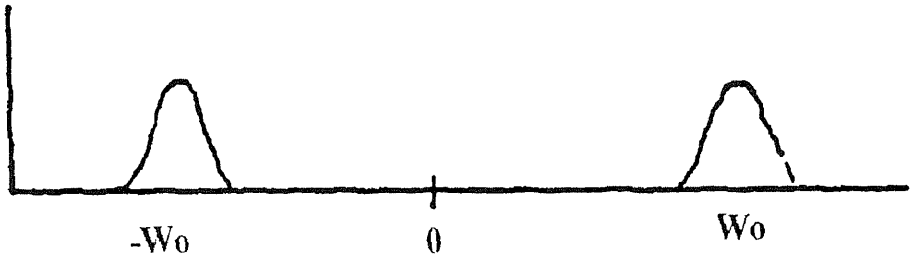


**Figure 1.5** Symmetry of energy density around the origin of a real signal

$$<\omega>=\int_0^{\infty}\omega\,|S(\omega)|^2 d\omega \qquad (14)$$

There were two approaches we could take. First, continue to consider real signals and when taking spectral averages integrate from zero to infinity rather than $-\infty$ to $\infty$. Second, define a new signal which has the same spectrum as the positive frequencies and zero spectrum for the negative frequencies.

The following method will describe how an imaginary signal was added to a real signal to form a complex signal[2]. In particular we want to write a complex signal of the form $z(t)= s(t) + js_i(t)$. By definition the analytic signal is one whose spectrum consists of positive frequencies. The standard method to form the analytic signal is to take the spectrum of the actual signal and delete the negative part of the spectrum and then form the complex signal by Fourier inversion. In particular, calculate $S(\omega)$ from the real signal s(t).

$$S(\omega)=\frac{1}{\sqrt{2\pi}}\int_{-\infty}^{\infty}s(t)e^{-j\omega t}dt \tag{15}$$

Then form the real part, s(t), of the complex signal, z(t), with the positive part of S(ω) only (equation 16). The factor of two was inserted so that the real part of the complex signal would be equal to the real signal we started out with.

$$s(t)=2\frac{1}{\sqrt{2\pi}}\int_{0}^{\infty}S(\omega)e^{-j\omega t}d\omega \tag{16}$$

The imaginary part of the complex signal, $s_i(t)$ turned out to be the Hilbert transform:

$$s_i(t)=\frac{j}{\pi}\int\frac{s(t')}{t-t'}dt' \tag{17}$$

For a simple harmonic signal described by s(t) = cosωt it was clear what the frequency was, but suppose we have a changing phase s(t) = A(t)cos(ϕ(t)). There have been many proposals for how to formulate the concept of instantaneous frequency. The generally accepted method was that it was the derivative of the phase of the analytic signal [2]. If the signal was written as $s(t) = A(t)e^{-j\varphi(t)}$ the instantaneous frequency was then $\omega_i=\varphi'(t)$.

## 1.2 Autonomic Nervous System

One system that changes rapidly in the human body was the autonomic nervous system (ANS)[8]. The autonomic nervous system (ANS) is made up of two functional divisions: the sympathetic (SMP) division and the parasympathetic (PSMP) division. These two divisions are anatomically, physiologically, and functionally distinct [9]. In general, the PSMP division enhances activities that gain and conserved energy, such as slowing the heart. The SMP division increases energy expenditures and prepares an individual for action by accelerating the heart . When SMP and PSMP nerves innervate the same organ, they often (but not always) have antagonistic effects. At rest there is considerably more parasympathetic activity to the heart than sympathetic.

The interplay of the SMP and PSMP outflow plays an important role in circulatory function. For the heart, sympathetic fibers terminate at the sinus node pacemaker, conduction system, atria, ventricles, and coronary vessels. While, parasympathetic fibers in the vagus nerve terminate at the sinoatrial and atrioventricular nodes, atrial and ventricular musculature, and coronary vessels (figure 1.6). Although inherent rhythmicity of the heart is due to a natural pacemaker situated in the sinoatrial node, continuous beat-to-beat control of heart rate is dependent on the relative balances between SMP and PSMP impulses delivered from the brain to the sinus node.

Factors other than the cardiac nerves can also alter heart rate (HR). The HR is also sensitive to changes in body temperature, plasma electrolyte concentrations and hormones. However, those factors are normally of lesser importance than the SMP and PSMP nerves to the heart [10].

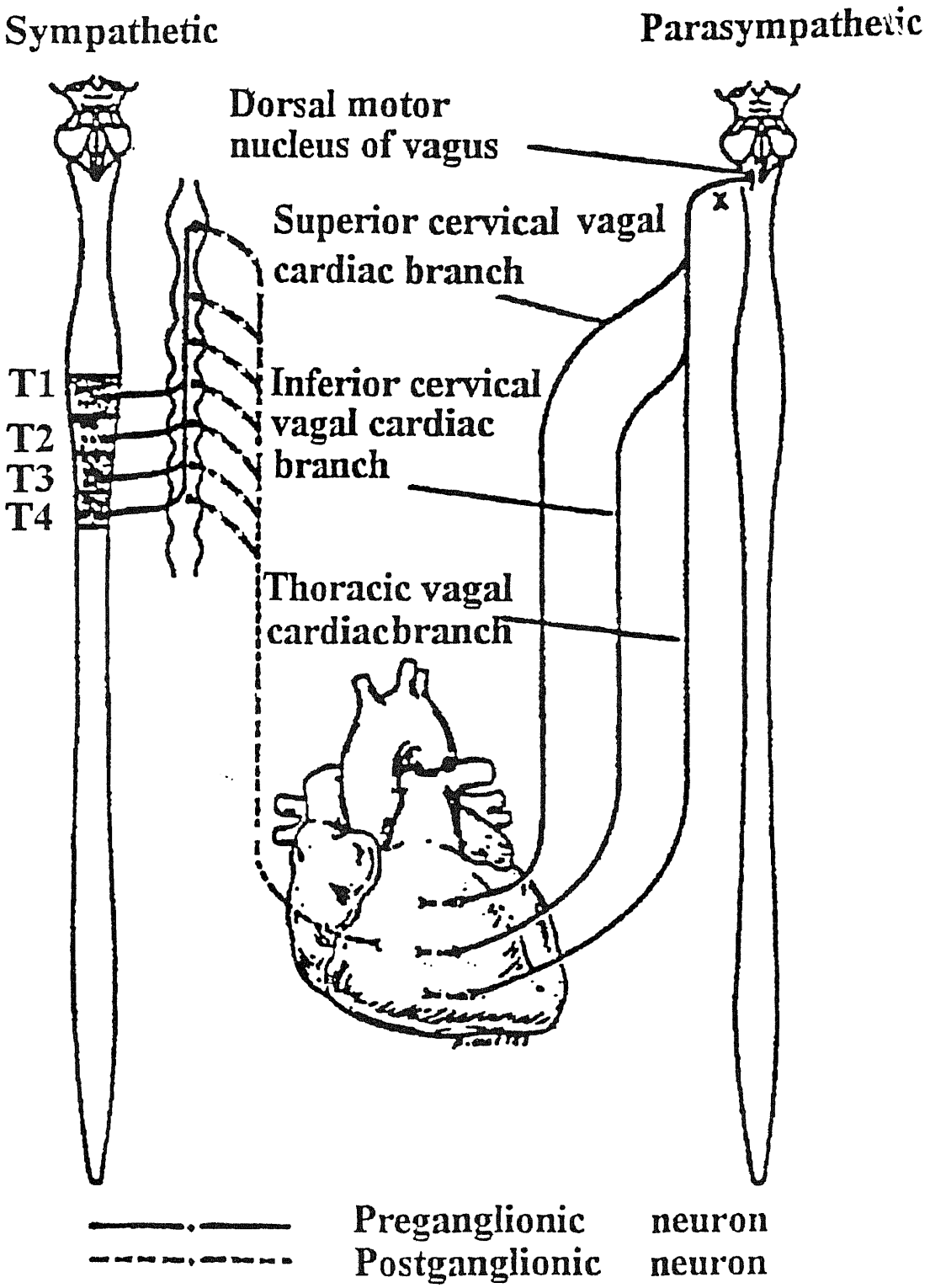


**Figure 1.6** Diagram depicting the nerve supply to the heart from both divisions of the ANS.

The ANS characteristically functions as a feedback control system. Although a central command controls overall autonomic behavior, several reflexes provide quick feedback to respond effectively to specific demands on the system. For example, high in the neck , each of two major vessels supplying the head ( the common carotid arteries) divide into two smaller arteries. At this division, the wall of the artery is thinner than usual and contains a large number of branching, vinelike nerve endings. This portion of the artery is called the carotid sinus. Its nerve endings are highly sensitive to stretch or distortion. Since the degree of wall stretching is directly related to the pressure within the artery, the carotid sinus serves as a pressure or stretch receptor, called the "baroreceptor" (figure 1.7).

An area functionally similar to the carotid sinuses is found in the arch of the aorta and is termed the "aortic arch baroreceptor." The carotid sinuses and aortic arch constitute the "arterial baroreceptor." Afferent neurons from them travel to the brain and eventually provide input to the neurons of the cardiovascular control centers.

The large systemic veins, the pulmonary vessels, and the walls of the heart also contain baroreceptors, most of which function in a manner analogous to the arterial baroreceptor. The primary control center for the baroreceptor reflexes is a diffuse network of highly interconnected neurons in the brainstem medulla called the "medullary cardiovascular center." The neurons in this center receive input from the various baroreceptors. This input determine the outflow from the center along axons that terminate upon the cell bodies and dendrites of the PSMP neurons to the heart and the SMP to the heart, arterioles, and veins. When the arterial baroreceptor

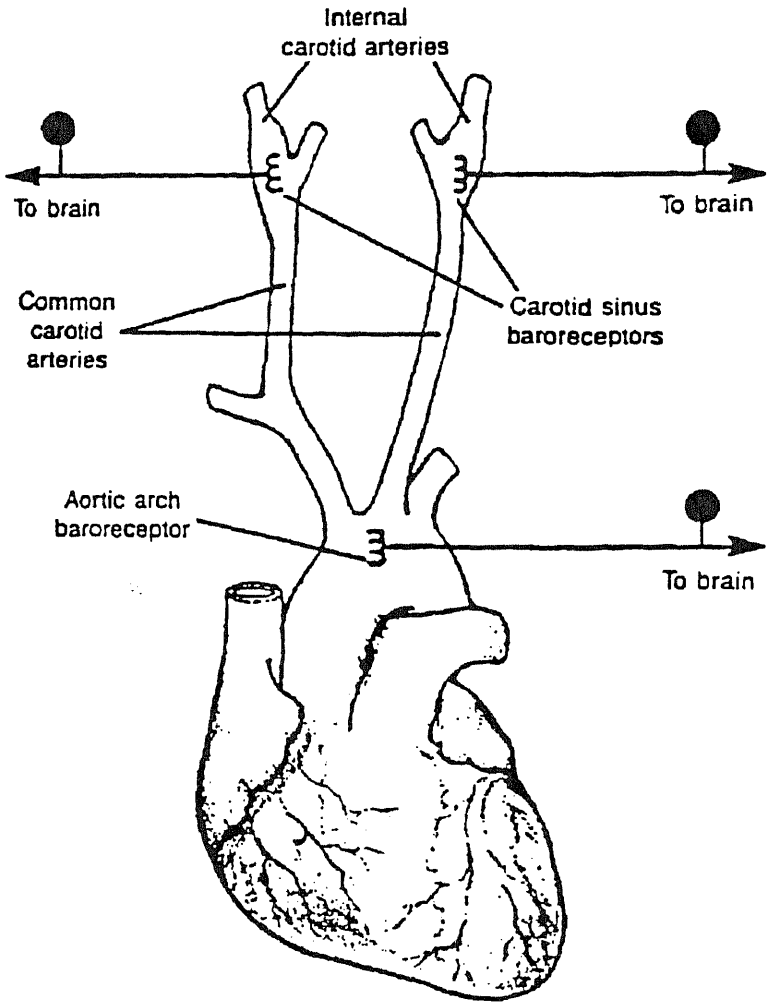


**Figure 1.7** Location of arterial baroreceptor.

increases its rate of discharge, the result is a decrease in sympathetic outflow to the heart, arterioles, and veins, and an increase in parasympathetic outflow to the heart. A decrease in baroreceptor firing rate results in the opposite pattern. The baroreceptor reflexes are short-term regulators of arterial pressure but adapt to a maintained change in pressure. Thus, in patients who have chronically elevated blood pressure, the baroreceptor continues to oppose minute-to-minute changes in blood pressure, but at a higher level [11].

### 1.3 Baroreceptor Reflex Sensitivity Index

The baroreceptor reflex sensitivity index (BRSI) is a marker of the baroreflexive control of blood pressure. BRSI is used to gauge the functioning levels of the different branches of the ANS[12]. BRSI is expressed as the slope of a regression coefficient line relating systolic blood pressure (SBP) and the cardiac cycle length. Thus, BRSI can be calculated from the ratio of delta R-R to delta SBP (expressed as ms/mm Hg).

The Valsalva maneuver has been shown to be an accurate indicator of baroreceptor reflex sensitivity [13]. The original Valsalva maneuver was described in 1704. It was a technique used for expelling pus from the middle ear. Later in 1851, an "imperceptible pulse" was described by Weber. This pulse can be related to the tachycardiac response that occurred during phase II of the Valsalva maneuver. Today the Valsalva maneuver is used clinically for the assessment of various cardiovascular disorders [14]. The Valsalva maneuver is a simple, non-invasive method of testing BRS since it can elicit significant rapid changes in heart rate, blood pressure, and

ECG [15].

The Valsalva maneuver is divided into four phases (figure 1.8 and Table 1.1) [16]. Phase I, a transient increase in systemic blood pressure with the onset of straining, reflects increased intrathoracic pressure. Phase II, a gradual decrease in pulse pressure and stroke volume due to a decrease in venous return, is often referred to as the active phase of the Valsalva maneuver. During phase III (initial release of straining) , the blood pressure transiently decreases further as a result of pooling of the blood in an expanded pulmonary vascular bed due to an abrupt decrease in intrathoracic pressure. This phase is rapidly followed by phase IV, characterized by an "overshoot" of the systemic pressure over baseline values. Each of these phases is accompanied by a specific reflex change in heart rate that was modulated by baroreceptor mechanisms. In figure 1.8 the vertical variation in the dark horizontal lines represent the interval between consecutive heart beats. This is called the interbeat interval (IBI) [17]. Reflex tachycardia occurs during the hypotension of phase II displayed as a decrease in the horizontal dashes showing the decreased distance between heart beats. Reflex bradycardia is associated with the over shoot (or hypertension) of phase IV. The horizontal lines increase denoting the increased distance between heart beats.

## 1.4 Heart Rate Variability: A Signature of Autonomic Function

Traditionally, the effect of the autonomic nervous system on heart rate has been investigated through two approaches. First, the average heart rate was measured under normal conditions as a reference, and then the average heart rate was measured

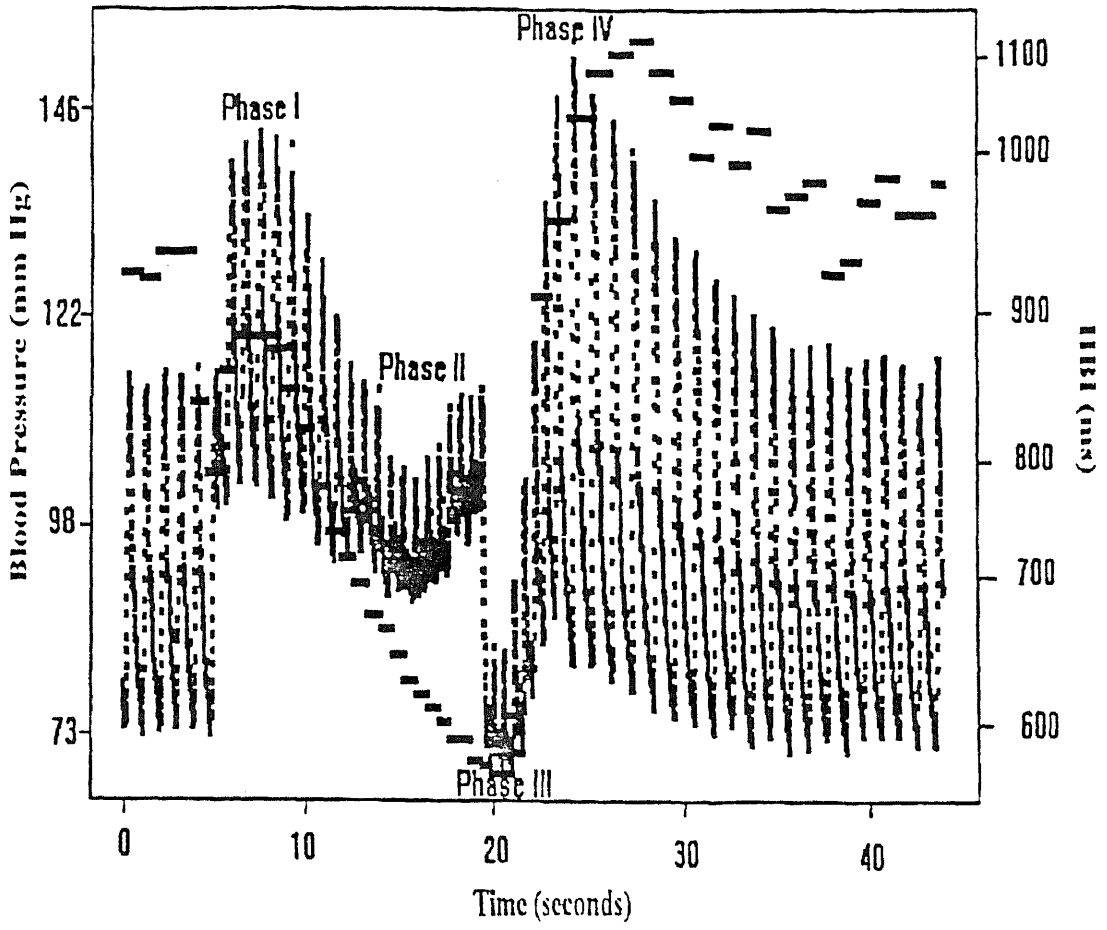


**Figure 1.8** Normal response to the Valsalva maneuver

Table 1.1 Four Phases of the Valsalva Maneuver

| Phase | Action | Blood Pressure | Pulse Rate |
|---|---|---|---|
| I | Onset of straining | Increases | Stable |
| II | Continued straining | Decreases | Increases |
| III | Release of straining | Decreases | Stable |
| IV | Continued release | Increases | Decreases |

under different drug treatments - atropine to block the parasympathetic nervous system and propranolol to block the sympathetic nervous system[18]. Recently, a second approach has used power spectrum analysis to analyze a biological rhythm such as heart rate, which consists of a time series of successive events, into a number of sinusoidal waves of different amplitudes and frequencies under different drug treatments [19].

From the drug studies three discrete frequency ranges were found to be of importance (figure 1.9) : a very low frequency range (VLF 0.02 to 0.06 Hz); a low

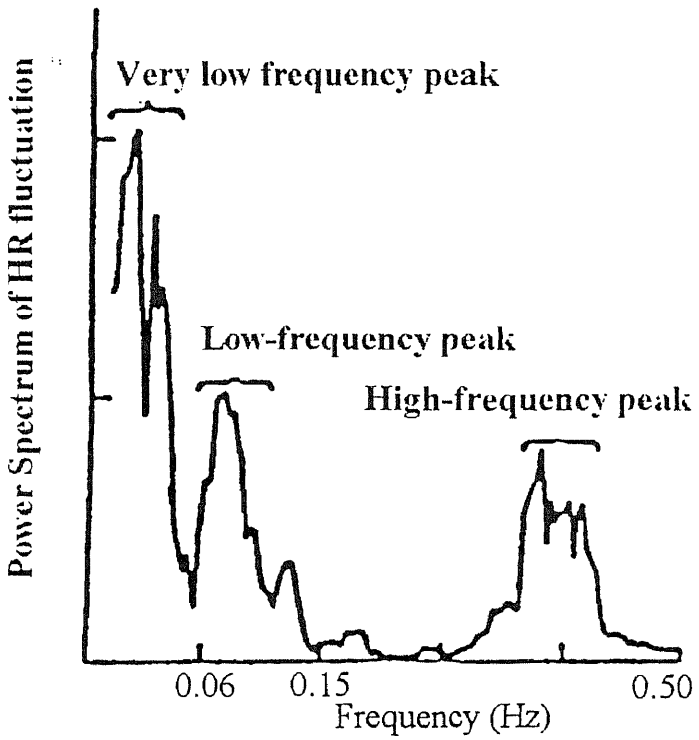


**Figure 1.9** Fourier transform of heart rate fluctuations, indicating very-low frequency, and high-frequency peaks. (From Akselrod, S. et al. Science,1981)

frequency range (LF, 0.06 to 0.15 Hz); and a high frequency range (HF, 0.15 to 0.40Hz) [19]. The very low frequency band was equated with the renin-angiotensin system; the LF band with blood pressure and baroreflex control; and the HF band with respiration. The HF band is mediated by parasympathetic pathways, while the LF band is mediated by both parasympathetic and sympathetic pathways. Parasympathetic blockade with atropine abolishes the HF heart rate fluctuations and substantially reduces the LF component. Additional propranolol further diminishes the LF band, but has an effect on the HF peak [20].

Assessment of parasympathetic activity from spectrum analysis is obtained via a measurement of the area under the HF peak . Sympathetic activity is less easy to quantify using this methodology. A better concept was that of "sympatho-vagal balance" which recognize both reciprocal and non-reciprocal parasympathetic and sympathetic influences on heart rate with a further measure, the LF:HF ratio [21,22].

## 1.5 Scope of Thesis

The aim of time-frequency analysis was to understand and develop the tools that can describe a time varying spectrum. In our research we have developed a tool to better understand the information contained in an interbeat interval signal. Expansion of the concept of spectral analysis of heart rate variability into time-frequency analysis gave us the ability to observe how the high frequency and the ratio of LF:HF changed as a function of time. For biological processes that are occurring very rapidly it was possible to understand and measure how the parasympathetic and sympatho-vagal balance changed. This was quantitatively assessed by taking the area under the HF

and LF ranges as a function of time from the time-frequency distribution. Such calculations were not possible without the utilization of time-frequency analysis.

Interbeat interval data were collected for various protocols. Normal and stroke subjects performed the Valsalva maneuver where ECG and continuous blood pressure data were collected. BRSI was calculated as a reference to gauge the severity of depressed baroreceptors and provide a tool for detecting impaired autonomic nervous systems. Time-frequency analysis was then applied before and after the maneuver to ascertain the changes in the autonomic system. The time frequency analysis of individuals with depressed baroreceptors were compared to those with normal baroreceptors. Time-frequency analysis was also applied to normal individuals performing an exercise test. The parasympathetic and sympatho-vagal changes were observed during rest, exercise and recovery.

Instantaneous frequency is the frequency that exists at a particular time. A paced breathing protocol was utilized to assess the validity of this measurement in understanding how the frequency content of the IBI changes during different rates of breathing. Instantaneous frequency was also utilized to study how electromyographic signals change during muscle fatigue experiments.

# CHAPTER 2

# METHODS

The following chapter documents the methods for acquisition of biological signals, experimental protocols and signal processing tools utilized for time-frequency evaluation of autonomic function. The biological signals acquired were respiration rate, interpolated interbeat interval, blood pressure, and metabolic activity. Experimental protocols consisted of baroreceptor reflex sensitivity evaluation, paced breathing, and exercise on both a kinetron and a bicycle. Signal processing tools were then used to derive clinically meaningful information for the biological signals collected during each protocol.

## 2.1 Acquisition of respiration

A RESP I impedance pneumograph (UFI, Morrow Bay CA) converted ventilation into an analog signal. The analog data were fed into a DAS-16 analog-to-digital converter (Keithley MetraByte/Asyst, Natick MA). The converted digital data then were stored on and IBM-compatible 286 computer with 2 Mb RAM and 170 Mb hard drive, using Streamer v3.25 data acquisition software (Keithley MetraByte/Asyst, Natick MA). Electrodes on each side of the thorax provided an indication of rate of ventilation by measuring the impedance of the tissue. The resistivity in the lungs changed in response to increased air in the tissue. Figure 2.1 displays a typical respiration curve from a healthy individual. The resistance increased during inhalation and decreased during exhalation.

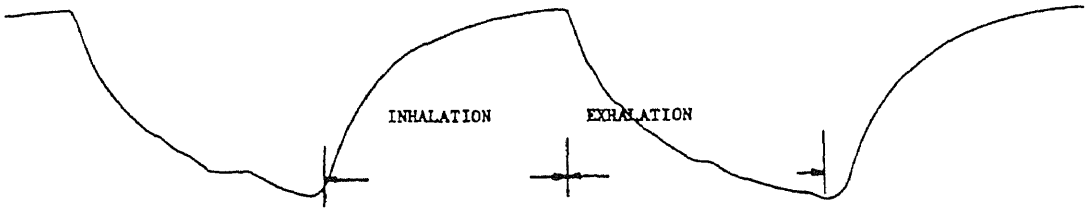


**Figure 2.1** Respiration recording.

## 2.2 Acquisition of InterBeat Interval

The electrocardiogram (ECG) was primarily a tool for evaluating the electrical events within the heart (figure 2.2). The first deflection, the P wave, corresponds to atrial depolarization. The second deflection, the QRS complex, is the result of ventricular depolarization. The final deflection the T wave, is the result of ventricular repolarization.

Figure 2.3 shows the standard bipolar limb leads for the ECG[26]. In lead I, the negative terminal of the electrocardiograph is connected to the right arm and the positive terminal to the left arm. In lead II, the negative terminal is connected to the right arm and the positive terminal to the left leg. In lead III, the negative terminal is connected to the left arm and the positive terminal to the left leg. The reference point (ground) is connected to the right leg.

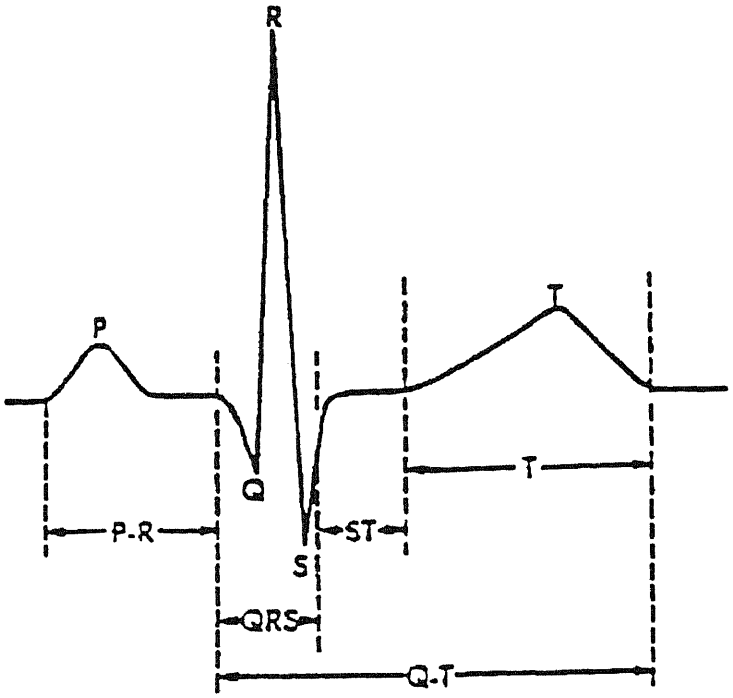


Figure 2.2 ECG complex

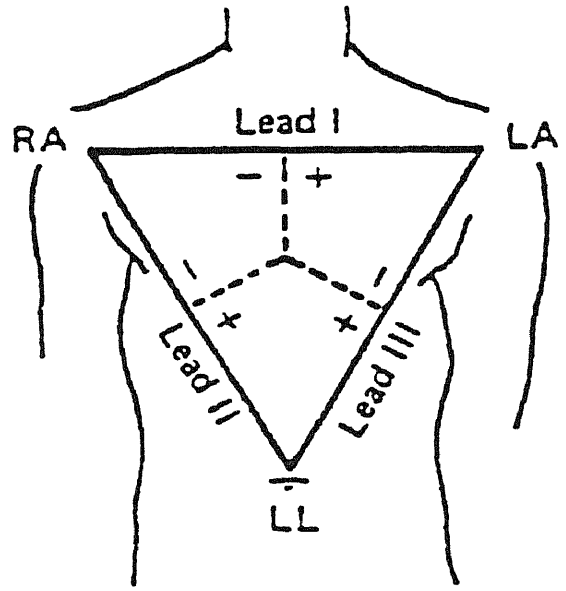


Figure 2.3 Standard bipolar limb leads of electrocardiogram.

Diagnostic ECG adhesive silver/silver chloride surface electrodes (Medtronic, Haverhill MA), connected by wire were placed on each subject to collect ECG data. The positive electrode was placed on the torso rather than on the left lower extremity in order to minimize electromyographic noise produced by the leg muscles during exercise. A good, low-resistance electrical connection between patient and electrode was essential for clean, interference-free ECG data. Failure to properly prepare the skin site caused base line shifts and noise from patient motion and respiration. Each skin site was prepared in the following manner: (1) The site was thoroughly rubbed with an alcohol swab. Then a dry piece of gauze pad was used to rub the site until it became slightly red. This removed the non-conductive outer layer of skin. (2) Application of the electrode to the prepared site was performed by running your fingers around the foam pad, smoothing it from the center out. This process was repeated for all sites.

A Q4000 monitor(Quinton Instrument CO., Seattle, WA) was used to acquire the ECG and detect QRS complexes. The QRS detection method in the Q4000 monitor was derived from leads I, II, and III. A rectangular pulse was created each time the QRS complex was detected (figure 2.4b). The resulting signal was then processed by a DAS-16 analog-to-digital converter (Keithley MetraByte/Asyst, Natick MA). The converted digital data was then stored on an IBM-compatible 286 computer with 2 Mb RAM and 170Mb hard drive, using Streamer v3.25 data acquisition software (Keithley MetraByte/Asyst, Natick MA).

The interbeat interval (IBI) represented the distance between two consecutive QRS complexes. Spectral analysis of heart rate variability was used to provide

estimates of the sympathetic and parasympathetic influences without drugs or other invasive procedures. The basic proposition behind these analyses was that the two autonomic branches influenced heart rate in a frequency-dependent way. Therefore,

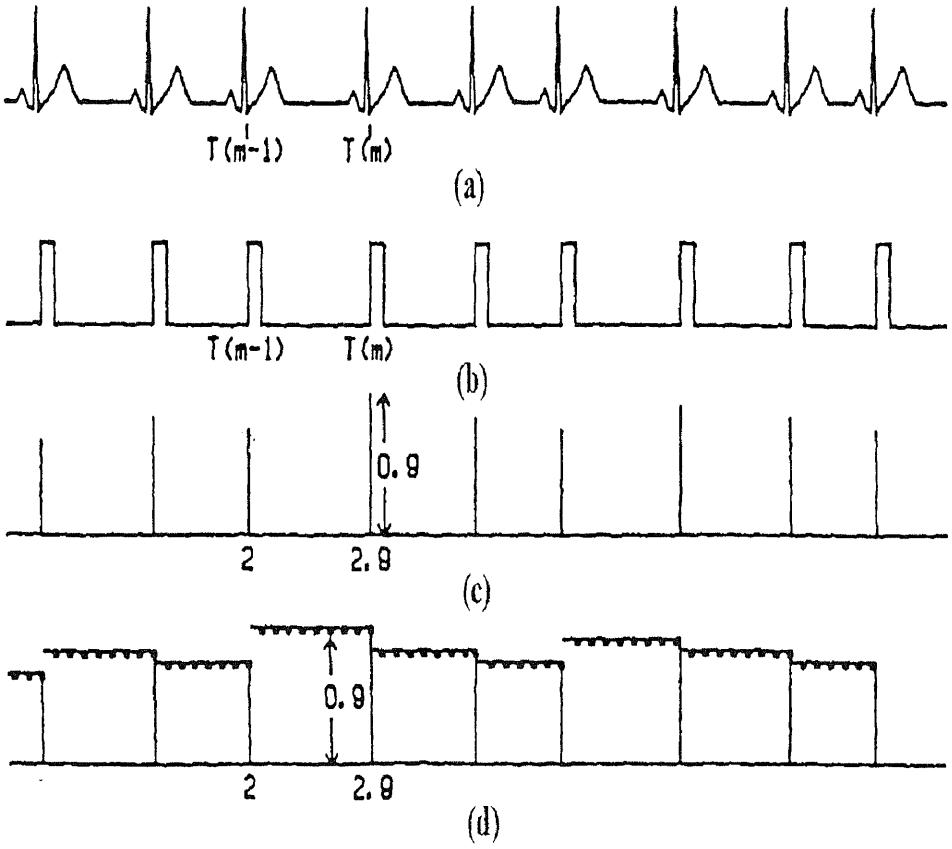


**Figure 2.4** (a) ECG signal (b) QRS pulse train (c) IBI values, (d) Interpolated IBI values (From Shin, Shaw-Jyh et al., "Assessment of Autonomic Regulation of Heart Rate Variability by Method of Complex Demodulation," IEEE Transactions on Biomedical Engineering, vol 36. Feb 1989)

the power spectrum of normal interbeat interval variability was characterized with two major, identifiable peaks through pharmacological studies. The best-known and best-defined peaks reflected changes in interbeat interval that cycle up and down at the same frequency as respiration. This respiration peak corresponds approximately to the well-known "normal sinus arrhythmia," and it was purely parasympathetic in origin [23]. In addition to the respiration peak, there was a low frequency peak that was mediated by both the sympathetic and parasympathetic systems.

The samples of the respiration signal were equidistant (0.1s apart); however, the IBI samples were not equidistant along the time axis since they occur whenever a QRS complex is detected. In order to produce equidistant IBI samples suitable for analysis and synchronized with the respiration signal, interpolation is needed. The method of backward step function interpolation [24] clearly showed the respiration frequency peak in the power spectrum of the interpolated IBI signal (figure 2.5) and was the easiest to implement. The method assumed that no new information about the course of the time series was available until the next heart beat had occurred. Therefore, all of the interpolated values between a beat at time T(m-1) and the next beat at time T(m) was set equal to the time difference between T(m) and T(m-1), which was the interbeat interval. For example, in figure 2.4c if a beat occurs at time 2sec and the next beat occurs at time 2.9sec, the interpolated values between time 2sec and time 2.9sec are all 0.9sec (figure 2.4d). The heart rate variability signal used in this work was this interpolated IBI signal.

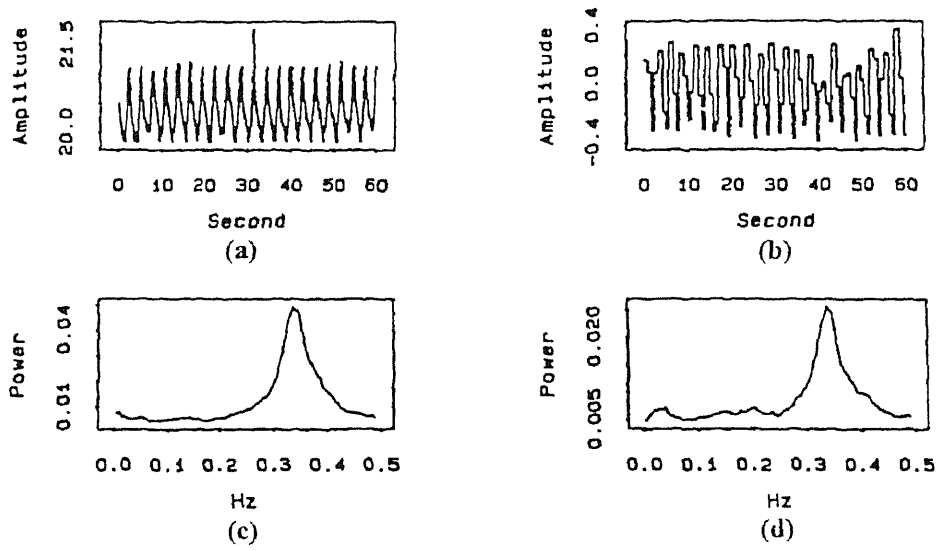


**Figure 2.5** (a) 60s respiration signal. (b) Corresponding 60s IBI signal. (c) Power spectrum of the respiration signal in (a). (d) Power spectrum of the IBI signal in (b). (From Shin, Shaw-Jyh et al. "Assessment of Autonomic Regulation of Heart Rate Variability by Method of Complex Demodulation," IEEE Transactions on Biomedical Engineering vol 36. Feb 1989).

## 2.3 Acquisition of Blood Pressure

Real-time pulse blood pressure data was collected as an analog signal using a Finapres Model 2300 Blood Pressure Monitor (Ohmeda, Englewood CO). Analog data was fed into a DAS-16 analog to digital converter (Keithley MetraByte/Asyst, Natick MA). The converted digital data was then stored on an IBM-compatible 286 computer with 2Mb RAM and 170 Mb hard drive, using Streamer v.3.25 data acquisition software (Keithley MetraByte/Asyst, Natwick MA).

This Finapres measures arterial blood pressure in the finger using a method

originally devised by Dr. Jan Penaz[25]. The 2300 Finapres monitor provided continuous measurement of finger arterial blood pressure displaying the pressure waveform, digital values of systolic, diastolic, and mean pressure as well as pulse rate and a time annotated trend display. To provide the dynamic response required to accurately measure the arterial pressure waveform, the cuff's pressure servo valve and pressure transducer were located in the patient interface module (figure 2.6).

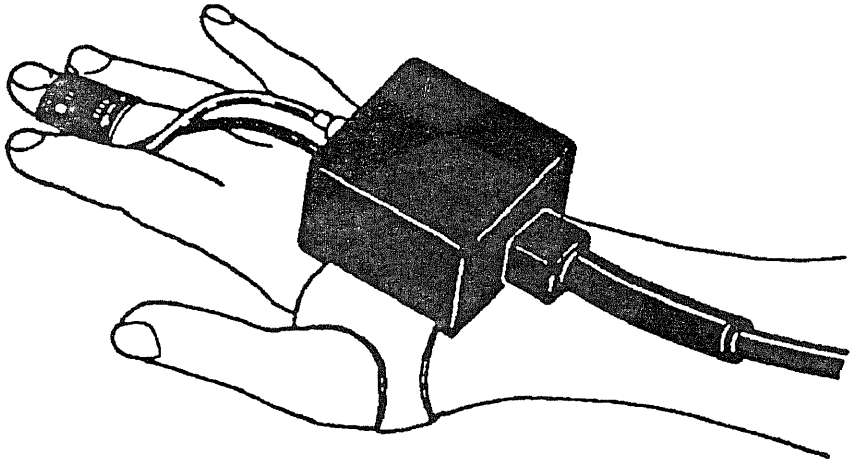

**Figure 2.6** Cuff and patient interface module mounted on the hand.(From 2300 Finapres Blood Pressure Monitor Operation Manual. Ohmeda CO. 1991)

The technique used an external pressure (the finger cuff) to equal the arterial pressure. When the external pressure equaled the arterial pressure the transmural pressure will be zero. With this technique the arterial walls would not change in size. The blood volume in these arteries would not change resulting in no change in the photoplethysmogram. A finger cuff containing photoelectric components for measuring blood plethysmography and a bladder for applying pressure to the finger was wrapped around the patient's finger and connected to the patient interface module. The blood volume was measured by a small photoplethysmograph located in the finger cuff (figure 2.7). Where the Penaz method used a constant pressure to "zero transmural pressure", the Finapres applied the reverse of this concept. The photoplethysmogram varied from the set point. A servo-valve caused a decrease or increase in the cuff pressure. This in return allowed for the photoplethysmogram to maintain a set point. The cuff pressure can be measured with an electric pressure transducer and the resulting signal displayed as arterial pressure. It was important to note that the manufacturer of the Finapres stated that the finger arterial pressure measured may not always reflect or correlate with the central arterial pressure [25]. However, it has been reported that blood pressure values obtained in this manner are comparable (+/- 4mm Hg) to those obtained using intra-arterial cannulas [26].

To optimize Finapres measurements the following should be observed: (1) The hand should be as relaxed as possible. (2) For best results use the cuff on fingers with good circulation. Fingers with poor circulation would produce low blood pressure values and dampened(rounded) waveforms. (3)Position the finger so that it was level with the patient's heart. If this was not practical, make the

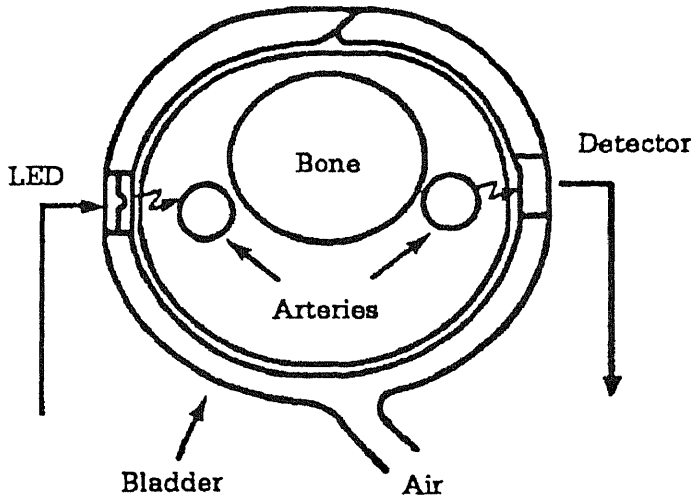


**Figure 2.7** Finger cross-section view illustrating optoelectronic components and bladder.(From 2300 Finapres Blood Pressure Monitor Operation Manual. Ohmeda CO 1991)

following correction:

-Subtract 2 mmHg from the blood pressure reading for each inch the finger was lower than the heart (-0.8 mmHg/cm)

-Add 2 mmHg to the blood pressure reading for each inch the finger was higher than the heart (+0.8 mmHg/cm).

The most common misapplication of the cuff was: (1) Incorrect orientation of the optoelectronic components (i.e. not on the sides of the finger) (2) Cuff wrapped too loosely or too tightly (3)Incorrect cuff size.

## 2.4 Acquisition of Volume of $0_2$/kg

Metabolic data was collected using the Q-Plex Cardio-Pulmonary Exercise System (Quinton Instrument Co. Seattle, WA). Subjects breathed through a #7900 two-way mask with low-resistance one-way valve (Hans-Rudolph, Kansas City MO). To collect metabolic data, the Hans-Rudolph mask was placed over the subject's mouth and nose and was secured using an elastic strap. The mask was connected to the metabolic data collection equipment. Gas analyzers were calibrated with commercially prepared gas mixtures to insure calibration. The microcomputer was calibrated before each subject was tested by inserting percentages of $O_2$ and $CO_2$ from standard gas samples, room temperature, relative humidity, barometric pressure, gas vapor pressure, and weight of the subject.

Metabolic data were collected by measuring over comparable metabolic equivalents (MET). As $V0_2$ is measured precisely using expired ventilatory gases, 1 MET is defined as the $VO_2$ expended at rest, and higher METs are defined as multiples of resting $VO_2$ (e.g. 2METs = 2 * resting $VO_2$).

## 2.5 Experimental Setup

Several signal processing methods were attempted on different experimental protocols to assess autonomic integrity and function. The baroreceptor reflex sensitivity index protocol was a noninvasive method of assessment of autonomic integrity. Time-frequency analysis was applied during protocols where heart rate changed either slowly or rapidly to study autonomic control of heart rate. The IIBI file produced during the paced breathing protocol represented slow changes in heart rate, whereas

the IIBI file produced during exercise represented a more dynamic change in heart rate. Two exercise protocols were employed to maintain equivalent exercise intensity for each subject. The exercise protocol on the kinetron employed the metabolic rate while the exercise protocol on the bicycle used heart rate to achieve equivalent exercise intensity for each subject. The time-frequency distribution represented a great deal of information and two methods were used to extract information from the distribution. The first used instantaneous frequency and the second involved the calculation of vagal tone and sympatho-vagal balance from the time-frequency distribution.

### 2.5.1 Baroreceptor Reflex Sensitivity Index

To measure BRS the Valsalva maneuver was performed. The Valsalva maneuver is a simple, non-invasive method of testing baroreflex sensitivity, as it can elicit significant rapid changes in heart rate, blood pressure, and ECG [15]. The subject was seated and diagnostic ECG adhesive silver/silver chloride surface electrodes were placed on each subject to record ECG and blood pressure data. The Finapres cuff and transducer were attached to the subject to obtain systolic blood pressure. The subject was instructed to blow into the sphygmomanometer and maintain an expiratory pressure of 40 mmHg for 15 seconds. Each subject performed three Valsalva maneuvers, separated by a rest period of 1 minute. ECG and blood pressure data were recorded two minutes before the Valsalva maneuver, during the Valsalva maneuver, and for one hundred and forty five seconds after the Valsalva maneuver.

### 2.5.2 Paced Breathing

A box was constructed where by a sequence of lights alternated between red and green lights at frequencies of 0.13, 0.20 and 0.30 Hz. Subjects in a seated position were asked to inhale during green light illumination and exhale during red light illumination. Breathing at those frequencies corresponded to 8, 12, and 18 breaths per minute (bpm). Two minute files containing ECG and respiration were collected while the subject performed the different rates of breathing.

### 2.5.3 Exercise Protocol on Kinetron

Exercise was performed on a Kinetron Exercise and Training System (Cybex, Ronkonkema, NY) which permitted varying degrees of isokinetic exercise. The position of the patient and speed of exercise were adjusted manually to select the energy requirements required to exercise. Data were collected and analyzed on 5 healthy control subjects (3 female, 2 male) , mean age 29.6 $\pm$ 9.0 years (range 23-43). Each subject was seated on the Kinetron. Expiratory gases were collected continuously todetermine $O_2$ and $CO_2$ fractions and to calculate each subjects' total body oxygen consumption ($VO_2$). The Finapres was connected to each subject to collect real-time pulse and blood pressure data. ECG data were collected as tolerated during rest, 2Met, 3Met, 4Met, 5Met. and normal relaxed breathing immediately following exercise (recovery) was also collected.

### 2.5.4 Exercise Protocol on Bicycle

The cycling protocol consisted of riding a cycle ergometer (Lifecycle, CA ) at 80

rev/min as dictated by the visual speedometer readout. The initial workload consisted of pedalling at 80 rev/min in an unloaded condition. Thereafter, the workload (resistance) was varied by a computer algorithm in order that the subject could maintain a heart rate of 70% of age predicted maximum. Age predicted maximum heart rate was calculated as 220 minus the age of the subject. The subjects sat on a bicycle for two minutes at rest and performed no physical activity. The subjects were then instructed to pedal comfortably for two minutes until their heart rate achieved 70 % of age predicted maximum. They maintained this pace for another four minutes for a total of 6 minutes of exercise. They were then asked to halt and rest without physical exertion for four minutes. ECG and respiration were collected in a continuous file of 12 minutes.

## 2.6 Data Analysis

### 2.6.1 Baroreceptor Reflex Sensitivity Index

The ECG and blood pressure data analysis were performed on an IBM-compatible 486/50MHz computer. The data analysis software package used was S-Plus for windows v3.1 (Statistical Sciences, Seattle WA), which includes modern statistical techniques and permitted the writing of custom S-Plus programs.

An S-Plus algorithm (see appendix C) was utilized to determine IBI. A software program was written to obtain the systolic values from the blood pressure curve. See Appendix A and C for details on BRSI calculation procedure and associated S-Pus Programs.

BRS was analyzed using methods previously described by LaRovere, [27]

which have been shown to be valid and reliable by Golstein [28]. BRS analysis utilized S-Plus for Windows data analysis software. ECG data were analyzed for detection of all sinus QRS complexes. Systolic blood pressure and R-R intervals were calculated as increments with respect to baseline measurements. The R-R intervals were plotted against the preceding arterial pulse as noted on the Finapres. Linear regression analysis was performed during the period between the beginning and end of the first significant rise in blood pressure of 20-30 mmHg. Change in blood pressure served as the independent variable, and change in R-R interval served as the dependent variable (figure 2.8). Regression lines with a correlation coefficient $\geq$ 0.80 were accepted for analysis. The slope of the line represented the baroreflex sensitivity index (BRSI), and was obtained by calculating the mean value of the three measurements. BRSI values below 3.0 msec/mmHg were considered to be "markedly depressed."

### 2.6.2 Instantaneous Frequency

Instantaneous frequency was the "average" frequency that existed at a particular time. It was calculated from the derivative of the phase of a signal, $\omega_i = \varphi/(t)$. The instantaneous frequency was also determined from the first conditional moment of the Wigner distribution.

$$\langle \omega \rangle_t = \frac{1}{|s(t)|^2} \int W(t, \omega)\, \omega d\omega = \varphi'(t) \qquad (2.1)$$

where $\varphi'(t)$ is the derivative of the phase of the signal $s(t) = A(t)e^{j\varphi(t)}$. An algorithm

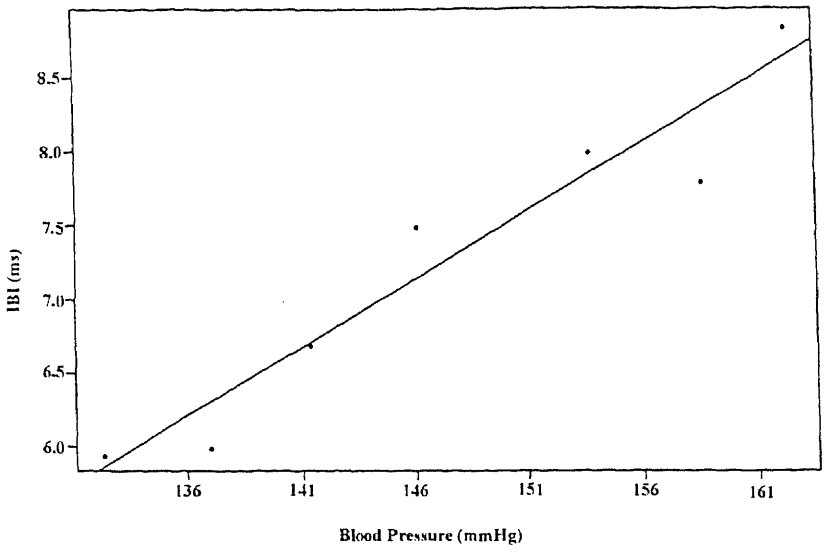


**Figure 2.8** Linear regression plot of systolic blood pressure vs. interbeat interval during phase IV of the Valsalva maneuver.

was written to calculate the instantaneous frequency form the Wigner distribution (see appendix C). The instantaneous frequency was calculated as a mean of extracting information about autonomic function from the Wigner distribution.

### 2.6.3 Vagal tone and Symptho-vagal balance via Wigner Distribution

The IBI was calculated using a program written in S-Plus (appendix C). It was then converted to an ASCII file that was loaded into Matlab. The very low frequency components contained in a signal [17] were sometimes an artifact caused either by the instruments used to acquire the signal or by such effects as movement. Those very low frequency components smear the power spectrum of the signal at low frequencies, and can smear the result of the processing. Therefore, the IBI was detrended using a

lowpass Butterworth filter with a cutoff frequency of 0.03Hz. Using the algorithm for the Wigner distribution the time-frequency analysis was performed. The area under the bands designating the LF and HF components was calculated for all time. See Appendix B and C for procedures and programs. The LF band corresponds to 0.05 to 0.15 Hz and the HF band corresponds to 0.15 to .040Hz. The symptho-vagal balance was determined from the ratio of the LF to HF components.

# CHAPTER 3

## RESULTS AND DISCUSSIONS

The following section presents the progression of research conducted on time-frequency analysis of biomedical signals. The first step was the verification of the computer software written to perform the Wigner distribution through artificially generated signals. After gaining an understanding of the parameters that affected the time-frequency distribution the first biological signal was tested.

Electromyographic experiments conducted on muscular fatigue at Kessler Institute for Rehabilitation provided data where the time-frequency nature of the signal was understood. As a preliminary test run of time-frequency analysis the data were tested and compared to the traditional time and frequency analysis used to quantify muscular fatigue.

After successful application of the computer software and the interpretation of the data from artificially generated signals and the electromyographic data our research efforts focused on heart rate variability. An assortment of heart rate variability data under various protocols was analyzed using time-frequency analysis. These protocols included paced breathing, exercise, and the implementation of the Valsalva maneuver. Observing significant qualitative differences in the measurement of the autonomic nervous system using time-frequency analysis on heart rate variability data prompted the development of techniques to quantify the results in a clinically meaningful way.

## 3.1 Computer Generated Signals

Two computer software programs utilizing time-frequency principles were tested. The first program performs the Wigner distribution and the second derives instantaneous frequency from the results of the Wigner distribution (see appendix C for computer programs). The time-frequency concepts governing the Wigner distribution and the instantaneous frequency have been discussed in chapter one.

Artificial signals were generated using Matlab which is an interactive software package developed for scientific and engineering computation. It integrates numerical analysis, matrix computation, signal processing and graphics. The computer program for generating a single component sinusoid is included in appendix C. Time-frequency representation of the sinusoid is displayed in figure 3.1a. The Wigner-distribution revealed that the single component sinusoid was composed of one frequency component that does not change throughout the file. The instantaneous frequency (figure 3.1b) also revealed that as time progressed the frequency at each instant of time was constant.

A more complicated artificial signal is the chirp. A "chirp" is a sinusoid where the frequency increases linearly with time (see appendix C for computer program to generate chirp). Figure 3.1c displays the results of the Wigner distribution on the chirp. The distribution shows that as time progresses the frequency content increases in a linear fashion. The instantaneous frequency of the chirp indicates that the frequency increases as a function of time. (figure 3.1d).

The computer program written to calculate the Wigner Distribution forms a matrix consisting of rows representing frequency and columns representing time.

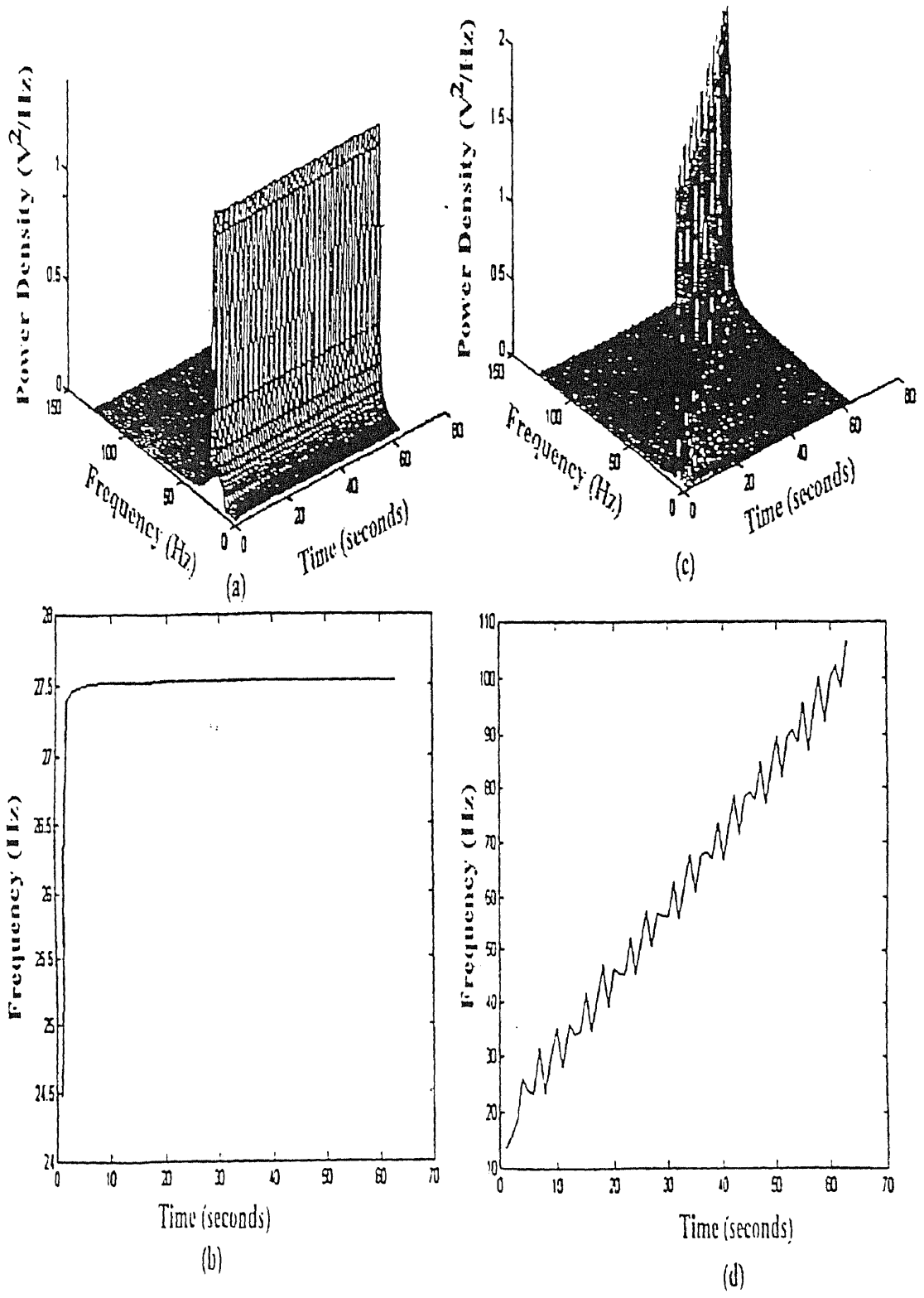


Figure 3.1 (a) WD of sine wave, (b) WD of chirp (c) Instantaneous frequency of (a) (d) Instantaneous frequency of (b)

Every cell defined by a row (frequency) and column (time) containes the amplitude of the frequency components present at that time. Each index representing the rows and columns may be translated to frequency in Hz and time in seconds. Manipulating the translation factor decreased or increased the resolution of the time-frequency distribution. The following two paragraphs will describe the methods used to convert index numbers to time and frequency and the role Fourier transform size, skip size and sample rate played in the process of time-frequency resolution.

Each column or time slice represented the frequency components present for a given segment of the signal. The Wigner distribution performed this calculation at the time of interest by multiplying a piece of the signal to the left with a piece on the right. If the Fourier transform size was chosen then the first time slice would occur at half the Fourier transform size in order to be able to multiply a piece of the signal to the left with a piece on the right. For example , if the Fourier transform size was 512 then the first time slice would occur at point 256 of the original signal. The next time slice was calculated by adding a number to point number 256. In the program used to calculate the Wigner distribution this parameter was called "skip". A typical number for skip in our applications was 25. For example, the second time slice would then occur at point 281 of the original signal which was 256+25 and the third at point 306 of the original signal which was 281+25. For each time slice the Fourier transform size remains the same. The last time slice does not correspond to the last point of the file but the point on the original signal that would allow multiplication of a piece of the signal on the left with a piece on the right. The number of time slices that may adequately be taken for a given Fourier transform size

and skip size was

# of time slices = (# of original signal points - Fourier transform size)/skip.

The corresponding real time value for each time slice = {1/2* Fourier transform size + (time slice)*(skip size)}/sample rate. Division by the sample rate converted points to seconds. For example, if we sampled data at 20 points/second with a Fourier transform size of 512 and a skip of 25 and wanted to know what time in seconds the third time slice corresponded to the calculation above would yield 16.6 seconds on the original time signal. The time resolution therefore was determined by the number of time slices calculated. By decreasing the skip size or the Fourier transform size the number of time slices would be augmented resulting in increased time resolution.

The rows of the matrix resulting from the Wigner Distribution represented frequency. Each row was in terms of an index number that was converted to frequency in Hz. In order to convert the index number we multiplied the index number by the ratio of the sample rate to the Fourier transform size. This ratio was called the "frequency resolution." By decreasing this ratio it was possible to increase the frequency resolution. For example, a sample rate of 20 points per second and a Fourier transform size of 512 yielded a frequency resolution of .039 Hz.

## 3.2 Electromyographic Signal

An electrode placed on the skin over the muscle fibers or within the muscle detects the electromyogram (EMG) signal, which is a summation of the motor unit action potential trains within its vicinity [29]. The electrical manifestation of the neuromuscular activation associated with a contracting muscle is called the EMG

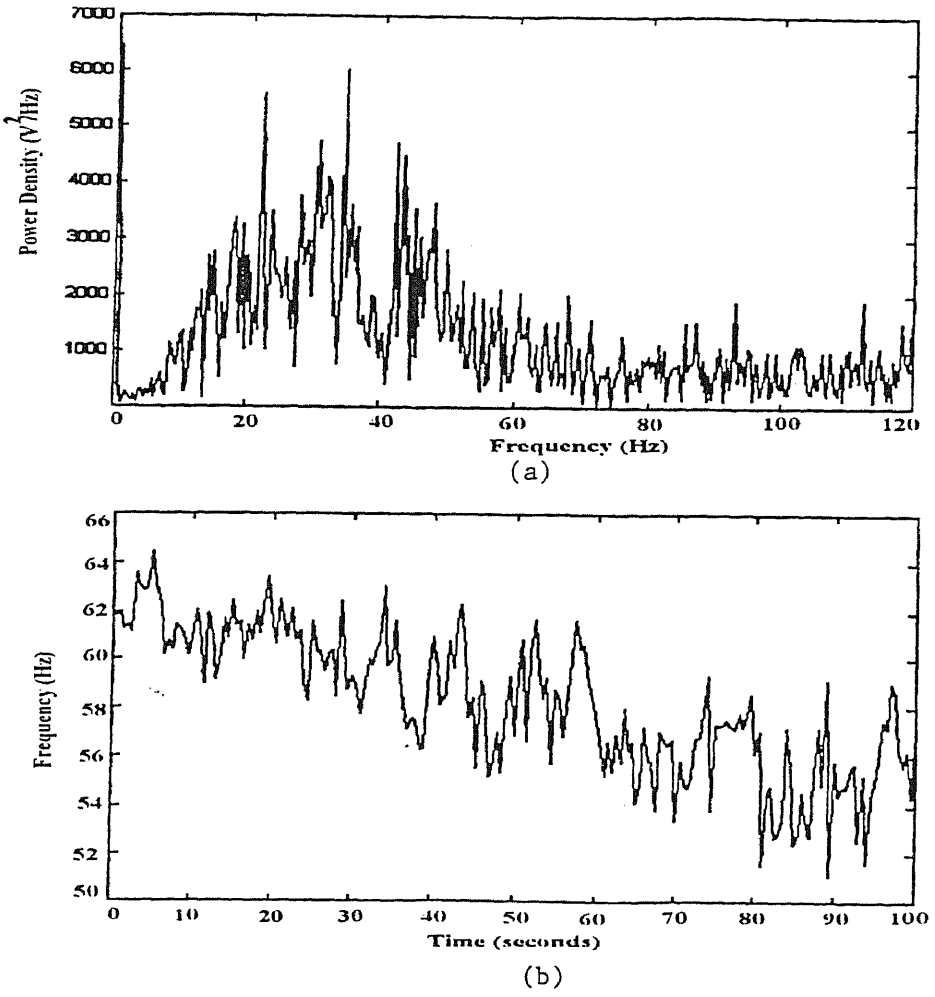


**Figure 3.2** (a) PDS of 5 seconds of surface EMG signal from the biceps brachii (b) Instantaneous frequency of 100 seconds of surface EMG signal from the biceps.

signal [30]. The amplitude of the EMG signal changes depending on the amount of muscle activity. Amplitudes vary from 50 microvolt to 1 millivolt, with frequencies ranging from 10 Hz to 3000 Hz, depending on the type of electrode, the placement of the electrode, and the activity of the muscle [31].

Two medical residents at Kessler Institute for Rehabilitation began a project to determine if the power spectrum obtained from fine wire electrodes could be used as an indication of muscle fatigue in the same manner that surface electrodes were used [32]. Muscular fatigue implied that as a contraction was held the muscle was weakening through time until failure (when the contraction can no longer be maintained) occurred. Muscular fatigue was associated with the inability to maintain the desired force output, muscular tremor, and localized pain [29]. The Fourier transform of five seconds of EMG data from the biceps brachii showed the distribution of energy versus frequency for the original signal. By squaring the amplitude of the frequency spectrum, the power density spectrum (PDS) was produced (figure 3.2a).

If the Fourier transform was applied to consecutive time sections of the original EMG signal, multiple power density spectrums were produced. The power density spectrum of the surface myoelectric signal compressed towards the lower frequencies during sustained muscle contraction [33]. This compression towards lower frequencies can be quantified. Many parameters values have been utilized, but the median frequency was the most popular. The median frequency was the frequency at which the area of the PDS was divided into two equal portions. The median frequency decreased with time during sustained isometric contractions. The

rate of decrease was higher when the contraction force was higher [29].

A method to apply time-frequency analysis to quantify the decrease of frequencies to the lower end was attempted. The Wigner distribution was applied to the entire EMG signal and the instantaneous frequency was derived (figure 3.2b). The instantaneous frequency was the frequency that exists at a particular instant of time. In order to compare median frequency with instantaneous frequency a least squared line was fitted to the median frequency plot and the instantaneous frequency plot. The slope of the least squared line fit for the median frequencies was -.15 Hz/sec and that for instantaneous frequency was -.1 Hz/sec. Only one file was tried since the goal of the project was to see if time-frequency analysis could be used as another method of quantifying the compression towards the lower frequencies during isometric contraction. Future research on the utilization of instantaneous frequency should shed light on its applications in the study of electromyographic signals.

### 3.3 Heart Rate Variability

The interpolated interbeat interval (IIBI) signal acquired from the ECG data revealed information about the role the autonomic nervous system (ANS) played in regulating the heart. The IIBI signal contained information about the spacing between consecutive R to R peaks which was regulated by the ANS. As mentioned in chapter one drug studies have shown that the areas under certain peaks of the Fourier transform of the IIBI signal were related to autonomic function. The high frequency range (0.15 to 0.40 Hz) was mediated by parasympathetic pathways, while the low frequency range(0.06 to 0.15 Hz) was mediated by both parasympathetic and

sympathetic pathways. Assessment of parasympathetic activity from spectrum analysis was obtained via a measurement of the area under the high frequency peak. Sympathetic activity was less easy to quantify using this methodology. A better concept was that of "sympatho-vagal balance" which recognized both reciprocal and non-reciprocal parasympathetic and sympathetic influences on heart rate with a further measure, the LF:HF ratio.

The spectral analysis of IIBI signals at best described the average parasympathetic activity or symptho-vagal balance. For situations where the ANS was changing very rapidly such an analysis technique was not adequate. Time-frequency analysis provided an improved way of looking at the information contained in an IIBI signal. Instantaneous frequency derived from the Wigner distribution of the IIBI could potentially extract information about the changes in the ANS. Variations in the HF range and the ratio of the LF:HF as a function of time was revealed using time-frequency analysis. The area under the time-frequency representation yielded the vagal tone or sympatho-vagal balance for every instant of time for a given signal. Besides serving as a qualitative tool in describing the influence of the ANS on the heart, quantitative measures were obtained to serve as possible clinical measures of ANS evaluation.

### 3.3.1 Detrending

The IIBI signals that were analyzed contained a very low frequency component (0-.03 Hz) due to baseline drift. As a result, the frequency ranges of interest were over shadowed by this large component. In order to eliminate this and to observe the

other frequencies that were present we utilized a digital lowpass filter. Infinite-duration unit pulse response (IIR) filters caused phase shifts which result in a time delay and transient responses at the beginning of the filtered data. This effect caused the whole time series to be shifted and some points at both ends of the data series were lost. Since our data series were time-locked during different trials, the results after filtering needed to have the same time periods as before filtering. To obtain a signal with precisely zero-phase distortion the data were filtered in the forward direction and then the filtered sequence was reversed and run back through the filter. Care was taken to minimize start up and ending transients by matching initial conditions. Such processing was required to maintain the integrity of the time signal after the low frequency component was removed.

### 3.3.2 Instantaneous Frequency of Paced Breathing

The first application of time-frequency analysis of heart rate variability involved the calculation of instantaneous frequency from IIBI signals obtained during paced breathing. Instantaneous frequency represented the frequency that was present at a particular time. As a first attempt at developing tools to extract the information hidden in an IIBI signal the instantaneous frequency showed promise.

Five healthy subjects ( range 20-45 years) were paced at 8, 12 and 18 breaths per minute. The Wigner distribution was applied to these IIBI files and the instantaneous frequency calculated. Figure 3.3 represented the instantaneous frequency of a subject during paced breathing. The instantaneous frequency varied slightly at the various pacing frequencies; however, the mean rate was at the

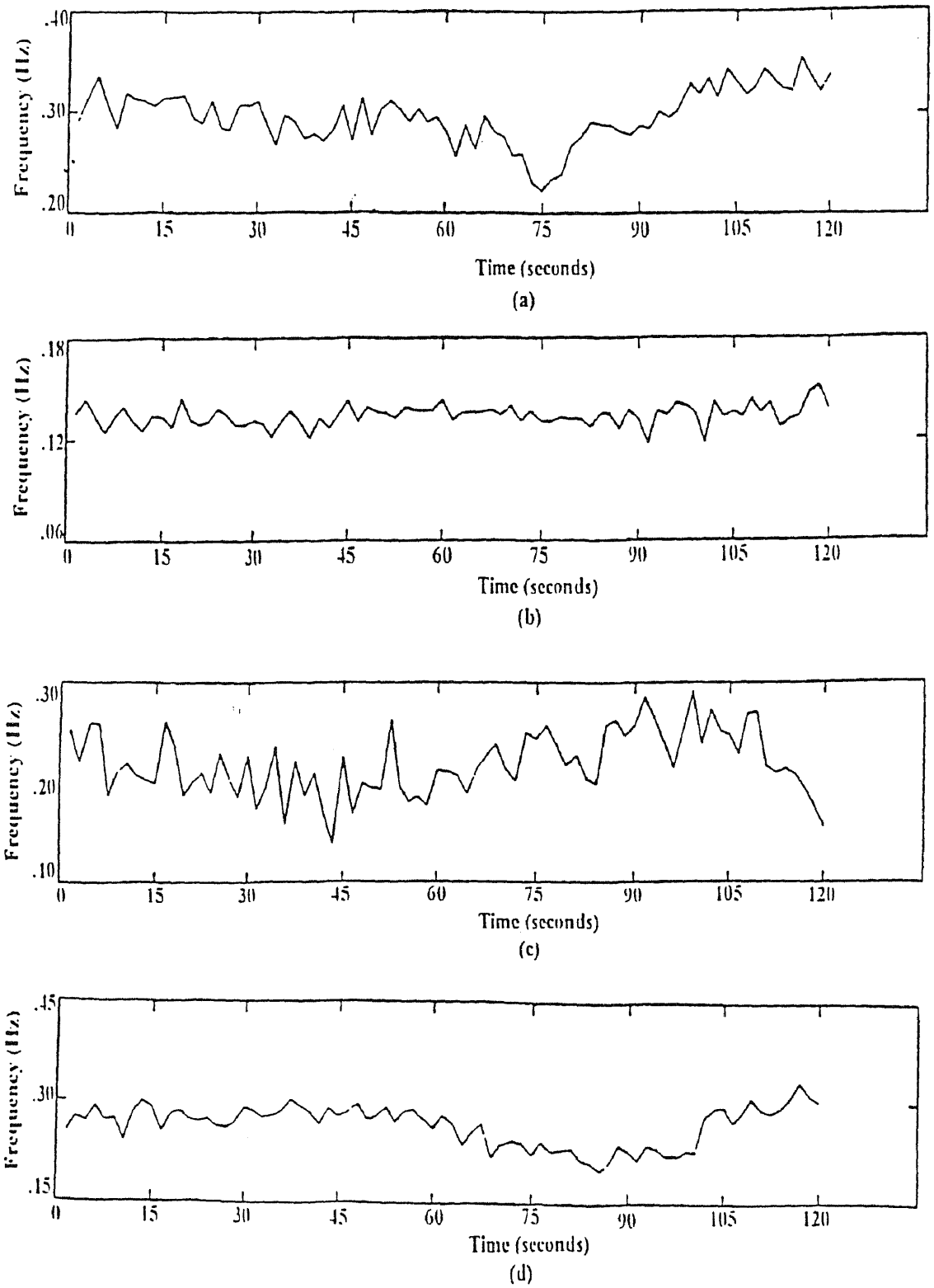


**Figure 3.3** Instantaneous frequency during (a) Rest, (b) Paced 8 (c) Paced 12 & (d) Paced 18

designated pacing. For example, the subject pacing at 8 breaths per minute (figure 3.3b) showed an instantaneous frequency hovering around 0.13 Hz. At the other rates of breathing the same correlation may be attained.

The paced IIBI signals were chosen because they were simple and the results easily interpretable. The analysis showed us that there were no errors in the processing of the IIBI signals since the results of the instantaneous frequency calculation correlated well with the breathing rates. The next step was then to apply time-frequency analysis to more complicated signals.

### 3.3.3 Vagal Tone via Wigner Distribution During Exercise on a Kinetron

The three dimensional time-frequency representation of an IIBI signal described the signal in time and frequency. However, extracting useful information from time-frequency analysis was an art combining engineering and physiology. In chapter one spectral analysis of IIBI signals was used to derive information on the activity of the ANS. The area under the HF range (0.15 to 0.40 Hz) was used as a measure of the functional state of the parasympathetic (PSMP) division. Time-frequency analysis allowed us to obtain more information than spectral analysis about the ANS. Spectral analysis only provided an average of the PSMP division for a given file. However, time-frequency analysis provided instantaneous change of the PSMP division. Since time-frequency analysis yielded the frequency components for each instant of time it is possible to calculate the area under the HF range for each instant of time. As a result, a measure of the activity of the PSMP was calculated for each instant of time.

Five subjects (range 20-45 years) were asked to exercise using the protocol for

the Kinetron described in chapter two. Six two minute files containing IIBI data were collected for each stage of the rest, exercise and recovery stages of the protocol. The Wigner distribution was applied to each file. The instantaneous vagal tone was calculated by determining the area under the HF range for each instant of time. Figure 3.4 contains the typical result of a healthy individual. The mean vagal tone decreased as the metabolic intensity (Mets) was increased. In figure 3.4b and 3.4c the mean vagal tone drops from 500 $V^2/Hz$ to 150 $V^2/Hz$ respectively as the metabolic consumption of $O_2$/kg was increased from 2 times normal to 3 times normal. A steady decline of parasympathetic activity was present as the consumption of $O_2$/kg was increased to 4 and 5 Mets (figure 3.4d and 3.4e respectively). After a two minute file at 5 Mets was collected the subject was asked to keep pedaling as the next file on the computer was prepared to acquire the transition from exercise to rest. This file was called the recovery file. The mean vagal tone at 5 Mets was 25 $V^2/Hz$ and the mean vagal tone during recovery was 150 $V^2/Hz$. The mean increase signified a return of the PSMP division to a resting state after exercise.

The change in the mean vagal tone derived from the Wigner distribution during the protocol corresponded with the vagal tone obtained through spectral analysis. However, time-frequency analysis allowed us to understand how the vagal tone varied during the two minute file. Every file in figure 3.4 showed fluctuations of the PSMP division during a particular stage of the protocol. These fluctuations represented changes in the PSMP activity as a function of time. Such information about the changes of the HF range were not available through spectral analysis.

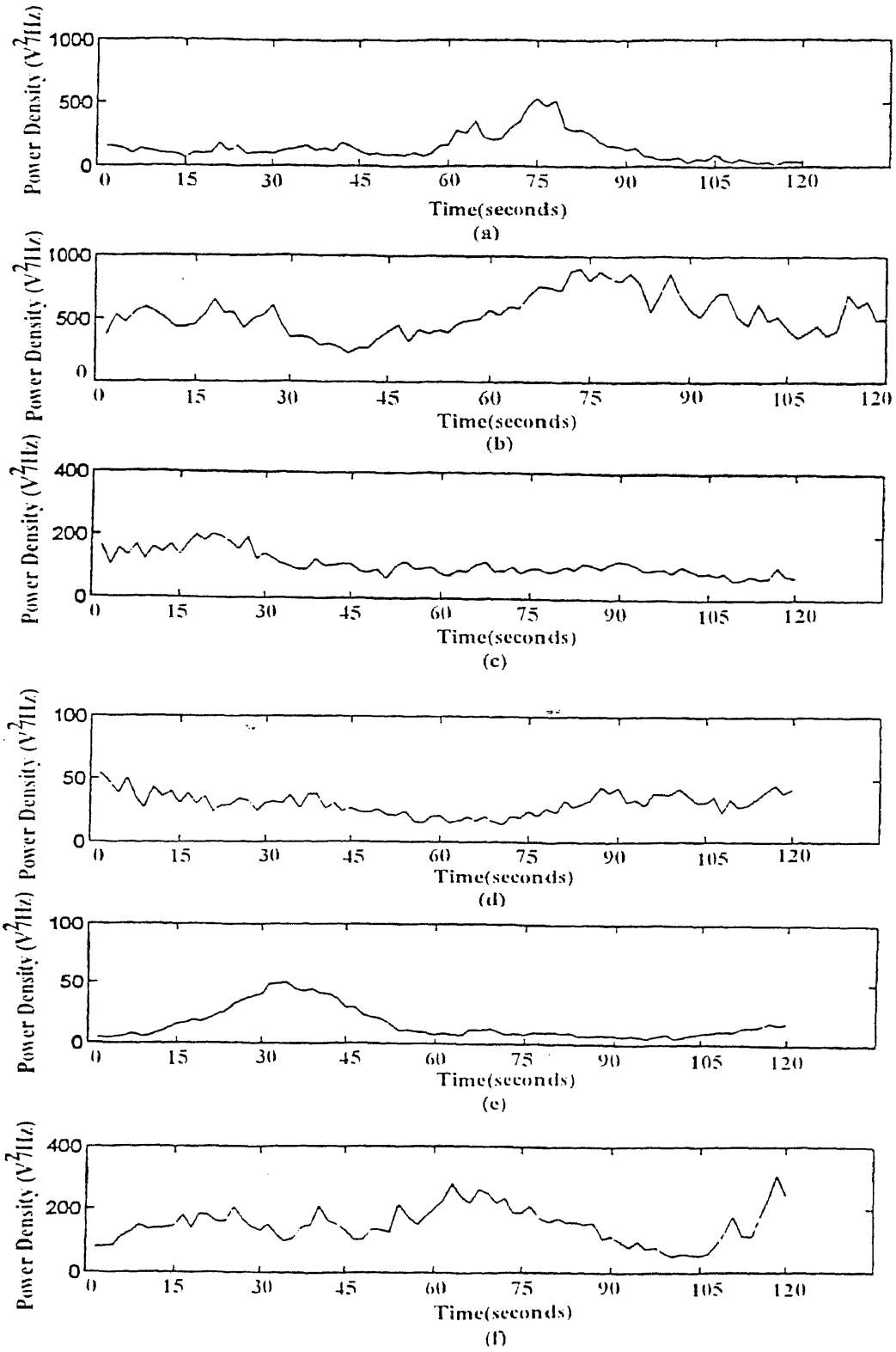


Figure 3.4 Vagal tone during (a) Rest, (b) 2 Met, (c) 3 Met, (d) 4 Met (e) 5 Met & (f) Recovery

### 3.3.4 Vagal Tone and Sympatho-Vagal Balance via Wigner Distribution during Exercise on a Bicycle

The time-frequency vagal tone study during exercise on the kinetron brought about an interesting question. Observing figure 3.4e and 3.4f the vagal tone increased dramatically from the end of the 5 Met file to the beginning of the recovery file, instead of a continuous change as would be expected. As a result, we believed that crucial information was lost during the transition. This observation was present for all subjects tested. In order to study the recovery utilizing time-frequency analysis a new protocol was designed using an exercise bicycle. The details of the protocol were discussed in chapter two. The protocol consisted of acquiring data two minutes prior to exercise (rest), six minutes of exercise at 70% of age predicted maximum heart rate and two minutes following the halt of exercise (recovery). The IIBI signal was acquired in a single file to prevent the loss of any information during the protocol.

The Wigner distribution was utilized to perform time-frequency analysis. The vagal tone was obtained for the entire file by calculating the area under the HF range for each instant of time. The symptho-vagal balance ( the ratio of the LF to HF range) was also obtained. As mentioned earlier drug studies had indicated that the LF range was a mixture of the activity of the sympathetic and parasympathetic divisions. The ratio was an indication of both reciprocal and non-reciprocal parasympathetic and sympathetic influences on the heart rate. Time-frequency analysis extended this concept of symptho-vagal balance so that for a given file the instantaneous change of this ratio may be calculated.

Ten subjects (range 19-53 years) were asked to perform the bicycle protocol described in chapter two. The Wigner distribution was applied to the IIBI signal and

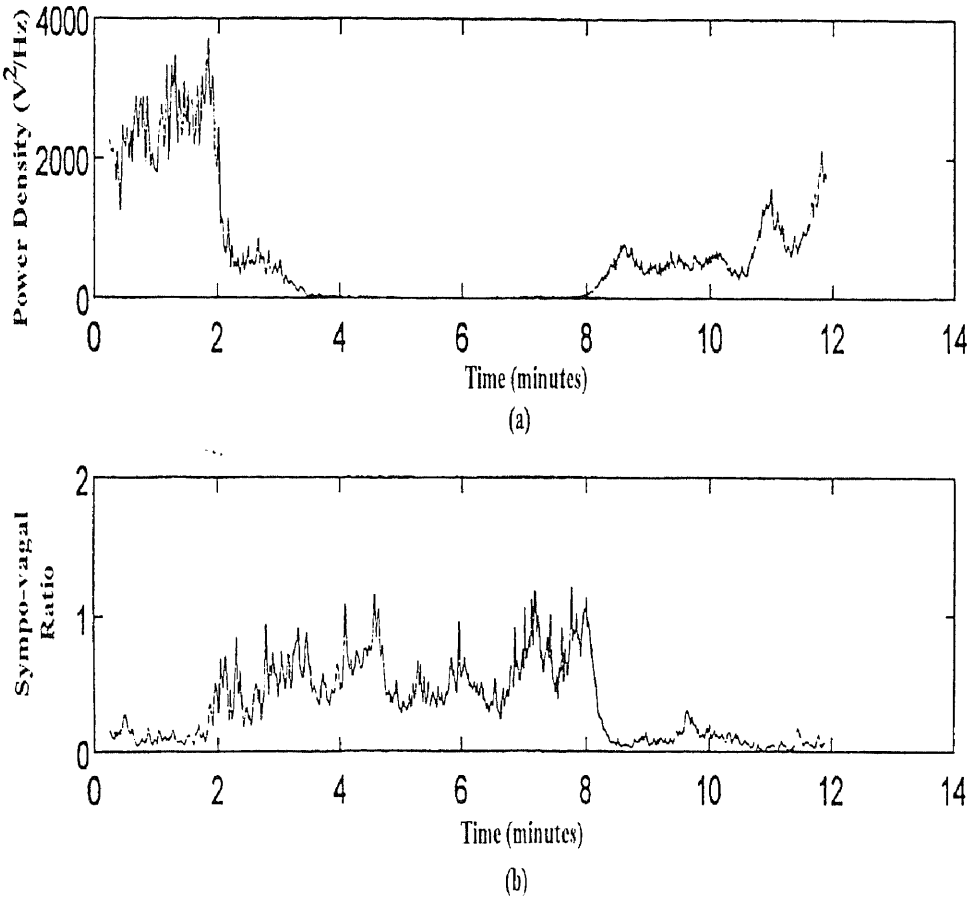


**Figure 3.5** (a) Vagal tone (b) sympatho-vagal balance, during 2 minutes of rest, 6 minutes of exercise and 4 minutes of recovery respectively.

the vagal tone and symptho-vagal balance calculated. Figure 3.5 displays the typical response of a normal healthy individual to the protocol. Figure 3.5a displays a drop of vagal tone as the subject initiated exercise at the two minute mark. During the six minutes of exercise the vagal tone activity was suppressed. At the eight minute mark the subject was asked to halt exercise and the vagal tone activity increased dramatically to normal levels. The rapid change in the vagal tone described through time-frequency analysis explained why there was such a drastic difference between the end of the 5 Met file and the recovery file in the pilot study conducted using the kinetron protocol. By the time the recovery file was prepared most initial changes were missed.

Since the exercise protocol on the bicycle was similar to the flight or fight response [34] we would expect a reciprocal relation to exist between the parasympathetic and sympathetic systems. Figure 3.5b displays the activity of the sympatho-vagal balance as a function of time. At the two minute mark where exercise began the symptho-vagal balance increased. The increased activity was maintained during the exercise session. When the subject was asked to halt exercise at the eight minute mark the symptho-vagal balance decreased to rest conditions. Observing the graphs in figure 3.5 it was evident that the reciprocal relations between the parasympathetic and sympathetic influences on the heart was depicted using this technique.

In all ten subjects the behavior of the vagal tone and symptho-vagal balance were similar. The qualitative significance of the visual depiction of the ANS warranted the design of techniques to quantify these changes. Several methods were

attempted to quantify the data. The first involved calculating the mean vagal and symptho-vagal balance for the three sections. These sections corresponded to rest, exercise and recovery. The second method to quantify the data involved calculating the area of the vagal tone and the symptho-vagal balance as a function of time for rest, exercise, and recovery. The last method involved calculating the slope of the transition from exercise to recovery. The results of these calculations for all ten subjects are summarized in table 3.1.

The mean vagal tone for each subject decreased from rest to exercise and then increased from exercise to recovery. The mean sympatho-vagal balance for each subject described a reciprocal relationship between parasympathetic activity and sympathetic activity. In all ten subjects the sympatho-vagal balance increased from a rest to exercise and decreased from the exercise to recovery.

The area under the vagal tone and symptho-vagal balance curves derived from the Wigner distribution depicted a similar relationship for all ten subjects. The vagal area decreased from rest to exercise and increased from exercise to rest. The sympatho-vagal area increased from rest to exercise and decreased from exercise to rest.

The slope of vagal recovery differed for each individual. However, a retrospective questionnaire inquiring the number of times an individual exercised per week revealed an interesting pattern in the data. The subjects who responded as having exercised at least three times a week had a slope of vagal recovery greater than 10 while those that did not had a slope below 10.

**Table 3.1** Quantitative Results from Time-Frequency Analysis of Exercise Protocol on Bicycle

| Subject | Age | Mean Vagal ($V^2$/Hz) | Area Vagal ($V^2$s) | Mean Sympo-Vagal ($V^2$/Hz) | Area Sympo-vagal ($V^2$s) | Mean Heart Rate (Beats/min) | Slope of Vagal Recovery ($V^2$) |
|---|---|---|---|---|---|---|---|
| S071994a | 19 | | | | | | 160 |
| Rest | | .84E3 | 600 | .16 | .10 | 56 | |
| Exercise | | .05E3 | 44 | .62 | .50 | 134.5 | |
| Recovery | | 3.0E3 | 2417 | .24 | .19 | 87 | |
| N071994a | 20 | | | | | | .57 |
| Rest | | 583.6 | 408 | .29 | .21 | 89 | |
| Exercise | | 28.0 | 22 | .47 | .38 | 131 | |
| Recovery | | 78.5 | 65 | .40 | .33 | 123 | |
| C071594a | 23 | | | | | | 1.7 |
| Rest | | 1.3E3 | 900 | .18 | .12 | 78.0 | |
| Exercise | | .03E3 | 24 | .55 | .44 | 135.0 | |
| Recovery | | .024E3 | 20 | .39 | .31 | 121 | |
| G071994a | 23 | | | | | | 20 |
| Rest | | 2.5E3 | 1750 | .14 | .10 | 58 | |
| Exercise | | .14E3 | 119 | .57 | .46 | 120 | |
| Recovery | | .46E3 | 367 | .18 | .14 | 98 | |
| D071994a | 26 | | | | | | 44 |
| Rest | | 2.3E3 | 1667 | .32 | .23 | 51.3 | |
| Exercise | | .18E3 | 144 | .64 | .51 | 119.3 | |
| Recovery | | 1.06E3 | 833 | .38 | .30 | 68.0 | |
| M072194b | 30 | | | | | | 10 |
| Rest | | .37E3 | 258 | .47 | .33 | 67 | |
| Exercise | | .075E3 | 61 | .48 | .38 | 118 | |
| Recovery | | 1.1E3 | 833 | .30 | .24 | 96 | |
| M072194a | 31 | | | | | | 83 |
| Rest | | 1.03E3 | 725 | .45 | .31 | 71 | |
| Exercise | | .04E3 | 36 | .70 | .56 | 126 | |
| Recovery | | 1.3E3 | 1042 | .25 | .20 | 89 | |
| K072594a | 43 | | | | | | 5 |
| Rest | | 491.9 | 350 | .55 | .39 | 62 | |
| Exercise | | 56.6 | 44 | .70 | .56 | 120 | |
| Recovery | | 265.6 | 216 | .30 | .24 | 89 | |
| S072594a | 53 | | | | | | 1.4 |
| Rest | | 892.7 | 633 | .35 | .25 | 94 | |
| Exercise | | 26.7 | 21 | .45 | .36 | 111 | |
| Recovery | | 71.2 | 57 | .26 | .20 | 104 | |
| R072294a | 53 | | | | | | 2 |
| Rest | | 608.0 | 433 | .33 | .24 | 64 | |
| Exercise | | 46.2 | 36 | .73 | .58 | 110 | |
| Recovery | | 164.5 | 133 | .40 | .325 | 94 | |

### 3.3.5 Time-Frequency Analysis of IIBI from the Valsalva Maneuver

The applications of time-frequency analysis up to this point dealt with signals from healthy normal individuals. Such an approach was taken to facilitate the development of the time-frequency processing techniques. Individuals with impaired ANS would have complicated the interpretation of the time-frequency results and placed doubt on the processing techniques. The confirmation of the results from time-frequency analysis of IIBI from paced breathing and the two exercise protocols in healthy individuals provided evidence that the proper signal processing techniques were being used. The next step was the application of time-frequency analysis to subjects that were impaired. In order to classify individuals with impaired ANS BRSI was calculated. Time-frequency analysis was then applied to the IIBI obtained during implementation of the Valsalva maneuver to categorize impaired ANS similar to the manner in which BRSI was utilized to characterize the extent of damage to the ANS.

Figure 3.6 is the normal response of a healthy individual to the Valsalva maneuver. During phase IV of the Valsalva maneuver the subject began to increase systolic blood pressure rapidly from a low of 80 mmHg to a high of 155 mmHg. As the heart rate began to decrease during continued release the IIBIs increased rapidly. However, this was not the case with a stroke survivor. Figure 3.7 demonstrates the response of a stroke survivor to the Valsalva maneuver. During phase IV the blood pressure increased rapidly from a low of 80 mmHg to a high of 200mm Hg as in the normal case but the IIBIs do not increase as rapidly. The heart rate takes longer to slow down and the IIBI intervals do not begin to increase until some time later.

The visual distinction between the response of a healthy vs. stroke may be

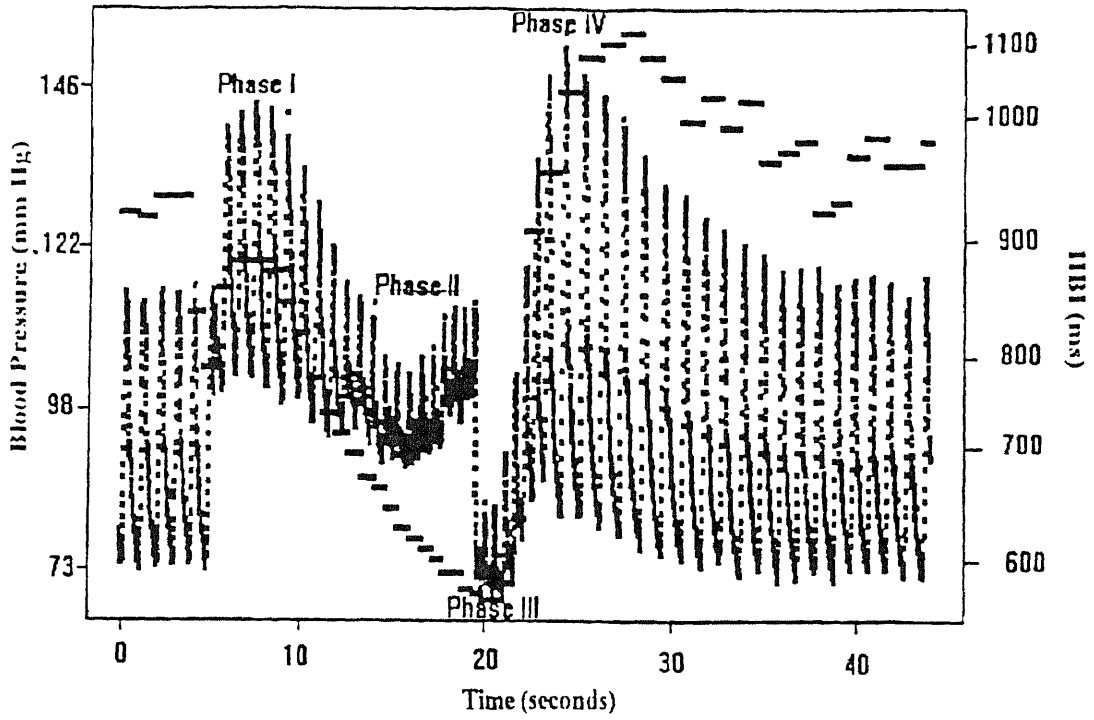


Figure 3.6 Normal response to the Valsalva maneuver

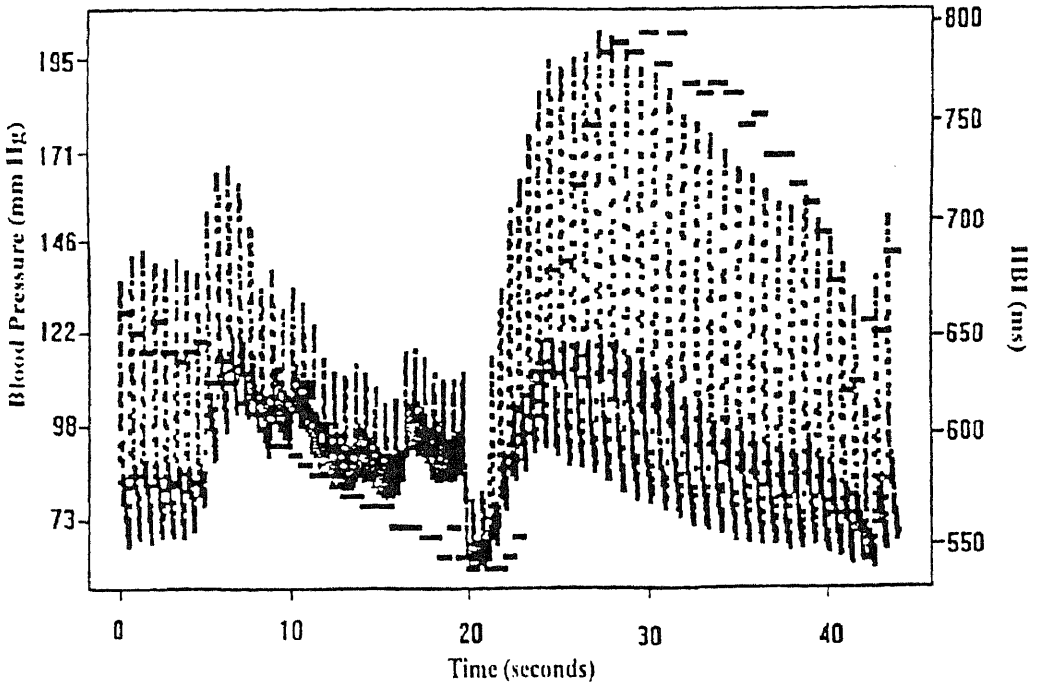


Figure 3.7 Stroke survivor response to the Valsalva maneuver.

quantitatively measured via the BRSI index. A pilot study was conducted where 5 healthy control subjects (3 female, 2 male) , mean age 26.6 $\pm$9.04 years and 5 stroke survivors (4 male, 1 female), mean age 53.0 $\pm$9.35 years were tested. The quantitative results of the study are shown in table 3.2. The mean BRSI in control subjects was 8.0 ms/mmHg and in stroke survivors, was 1.5 ms/mmHg. Using analysis of variance (ANOVA), a significant group effect was observed ($p=0.024$). All normal BRSI were above 3.0 ms/mmHg and all stroke survivors were below 3.0 ms/mmHg denoting clinically a depressed ANS.

Time-frequency analysis was applied to four stroke survivor (range 41-64 years) and four healthy individuals (range 40-55 years). The analysis began at the highest IIBI value to measure the recovery of the ANS of normals vs. strokes. From qualitative observations the vagal tone dropped in all cases after the highest IBI was achieved. However, the time it took various individuals to return to homeostasis was not the same. Various attempts were made to measure the drop of vagal tone from the highest IIBI value. The difference between the initial vagal tone and the final was calculated. A percentage drop was also determined and the slope of the vagal drop was assessed using a least squared line fit. There also existed a delay before the vagal tone began to drop. The length of this delay was also calculated. The results of these calculation are presented in table 3.3.

The vagal drop, % vagal drop, slope of vagal drop and delay before vagal tone drop between stroke survivors and normals did not show any patterns of difference between the two populations. One possible reason could be that the subjects were not age and sex matched resulting in the varied pattern obtained. A second reason could

Table 3.2 Baroreceptor Reflex Sensitivity Index of Normal vs. Stroke Survivors

| Normal Subjects | | | | | |
|---|---|---|---|---|---|
| Subject Age/Sex (M/F) | 23/F | 23/F | 24/F | 35/M | 43/M |
| BRSI: Valsalva maneuver (ms/mmHg) | 3.89 | 6.35 | 5.41 | 16.77 | 7.18 |
| Stroke Survivors | | | | | |
| Subject Age/Sex (M/F) | 53/F | 41/M | 47/M | 60/M | 64/M |
| BRSI: Valsalva maneuver (ms/mmHg) | 2.55 | 1.04 | 1.80 | 1.95 | 0.21 |

Table 3.3 Time-Frequency Analysis of Post Valsalva between Stroke and Normal

| Subject | Vagal Drop ($V^2$/Hz) | % Vagal Drop | Slope of Vagal Drop ($V^2$) | Delay (s) |
|---|---|---|---|---|
| BV51126 | 293.3 | 78 | -5.16 | 41.5 |
| H12138 | 52 | 21 | -2.33 | 27.8 |
| G12228z | 340 | 16 | -3.28 | 28.1 |
| K12237 | 592.5 | 24 | -12.1 | 29.2 |
| R050294a | 301 | 60 | -6.9 | 25.3 |
| K050294a | 557 | 80 | -7.3 | 36.1 |
| D050494a | 1.38E4 | 94 | -200 | 21.55 |
| H050494e | 237 | 53 | -3.8 | 16.5 |

be that a large enough population was not tested to reveal any significant findings. Further research is required in order to assess the usefulness of time-frequency analysis of phase IV of the Valsalva maneuver as a predictive indicator of autonomic function impairment.

# CHAPTER 4

# CONCLUSIONS

Spectral analysis of heart rate variability was used to provide estimates of the sympathetic and parasympathetic influences without the use of drugs or invasive procedures. However, there were many situations where heart rate changed rapidly over time and the control of those changes by the autonomic nervous system (ANS) was of considerable interest. Calculation of vagal tone and sympatho-vagal balance from the time-frequency distribution described the changes of parasympathetic and sympathetic influences on heart rate.

## 4.1 Vagal Tone and Sympatho-vagal Balance via Wigner Distribution

The time-frequency distribution of an interpolated inter-beat-interval (IIBI) signal attained during rapid changes of heart rate represented a complicated signal. For example, figure 4.1 represents the Wigner distribution for the IIBI attained during exercise at 3 Mets. The distribution contains a lot of information but the problem arose in extracting the information in a clinically meaningful way.

Several methods were attempted to extract information from the Wigner distribution. Two methods attempted were filtering techniques and calculation of instantaneous frequency. Filtering the IIBI data removed a direct current (dc) trend from the time-frequency distribution but did not yield clinically relevant interpretations. Calculation of the instantaneous frequency of the IIBI from paced

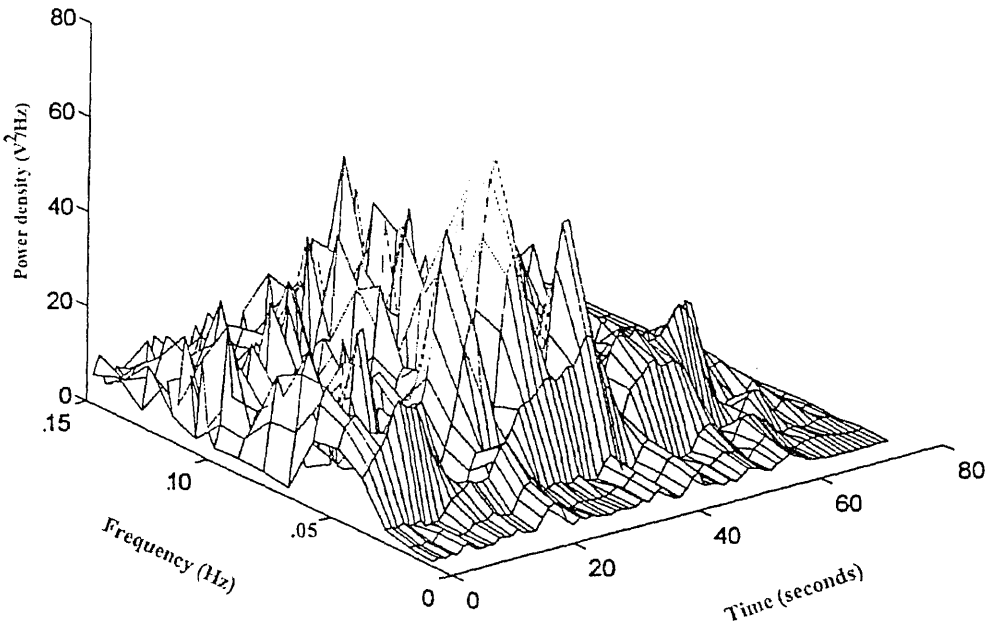


**Figure 4.1** WD of IIBI attained during exercise at 3 Mets.

files showed a correlation between the respiratory rate and the frequency of the IIBI. When applied to IIBI signals attained during complex protocols such as exercise the instantaneous frequency did not correlate with any physiological interpretations. Therefore, other methods were attempted to derive information from the Wigner distribution.

The expansion of the concept of spectral calculation of vagal tone and sympatho-vagal balance to time-frequency produced significant clinical findings. Vagal tone is the assessment of parasympathetic activity from spectrum analysis by measurement of the area under the high frequency peak. Time-frequency calculation

of vagal-tone estimated how the parasympathetic activity varied as a function of time. Similarly the smypatho-vagal balance recognized the reciprocal parasympathetic and sympathetic influences on heart rate through the ratio of low frequency to high frequency. Time-frequency calculation of the sympatho-vagal balance indicated how this ratio changes as a function of time.

The calculation of vagal tone and sympatho-vagal balance via time-frequency analysis provided information not obtained from spectral analysis. First, time-frequency analysis described vagal tone and sympatho-vagal balance as a function of time. Second, the slope of vagal tone and sympatho-vagal balance provided a means of assessing autonomic integrity. Finally, time-frequency analysis of heart rate variability indicated a means of assessing mental state. In rest files where the anxiety level was low vagal tone increased (figure 4.2). However, in pre-Valsalva files where the subject was anticipating the initiation of the Valsalva maneuver the vagal tone decreased (figure 4.3).

## 4.2 Baroreceptor Reflex Sensitivity Index

Baroreceptor reflex sensitivity index was one method of categorizing patients suspectable to cardiac complications. However, it should not be used as the sole method of assessing patients prone to cardiac infarctions. With other measurements such as heart rate variability (HRV) the two add strength to predicting a patient's susceptibility to cardiac abnormalities.

A longitudinal study conducted on stroke patients indicated that they had a fifty percent likelihood of suffering a heart attack [35,36]. During rehabilitation

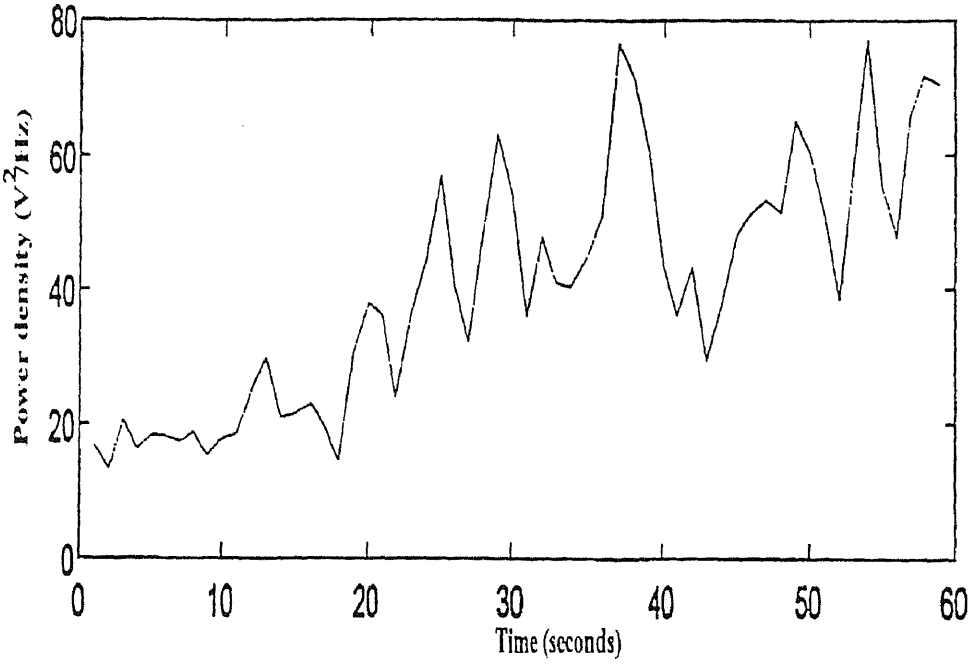


Figure 4.2 Vagal tone via WD of rest file.

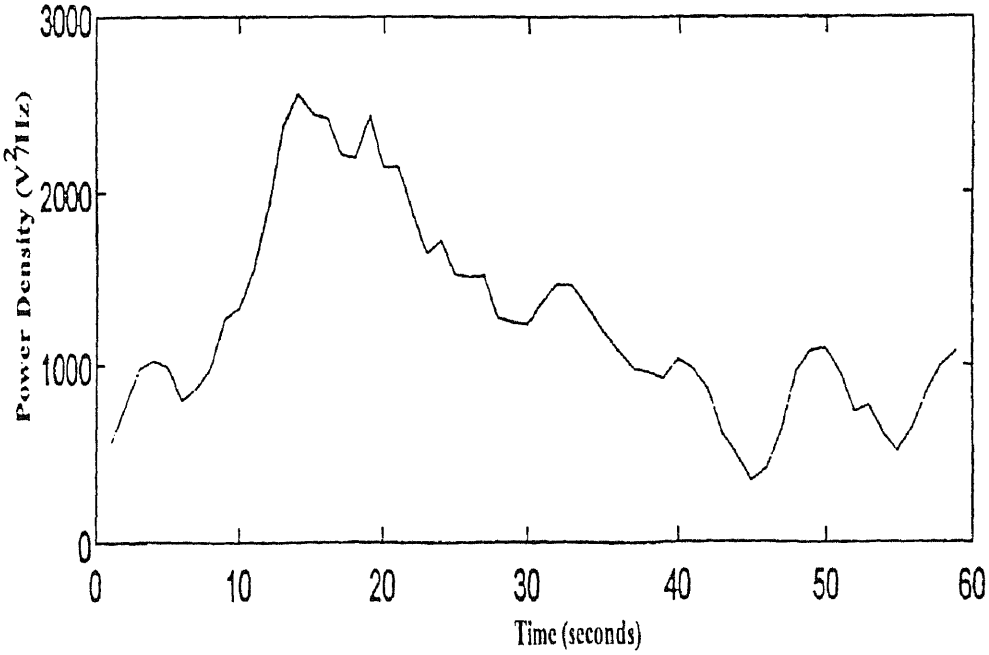


Figure 4.3 Vagal tone via WD of pre-Valsalva maneuver

stroke patients may perform activities that are strenuous and in some cases lead to a heart attack[37]. If there are non-invasive methods of assessing this, better care may be taken in rehabilitating such patients who are at a greater risk. We looked at BRSI as a means of categorizing stroke patients at risk for myocardial infarctions.

The pilot study on BRSI indicated that there was a drastic difference between normal subjects and stroke survivors. The BRSI of those surviving a stroke was less than the threshold for normal subjects. However, it must be stated that the study was a pilot study and contained room for improvement. First of all the study was not age and sex matched. In future research of BRSI age and sex matched individuals will be tested. Second, a larger population should be tested. In our short study stroke patients showed a depressed BRSI. As a predictive indicator of myocardial infarction these subjects would be categorized as at a high risk for myocardial infarction. The only way to verify this would be to conduct a longitudinal study where by BRSI values were obtained over a longer time span. However, there will be stroke survivors whose BRSI will not be lower than the threshold for depression. The only way to verify predictability of the test would be to conduct a longitudinal study.

The implications for BRSI is wide spread. BRSI has been shown to be useful in other patient populations such as diabetes[38]. With a method of risk categorization it is possible to tailor treatment to stroke patients. Individuals with a low BRSI may be given medication and less strenuous exercise in order to help them increase BRSI. BRSI is one measure of the autonomic nervous system and combined with others it will serve as a strong clinical tool in the treatment of a stroke patient population.

## 4.3 Future Work

The possibilities of risk categorization of individuals with possible cardiac complications is a benefit to the patient and the physician.. The techniques and methods have been designed to carry out the signal processing. The next step is the designing of a protocol to answer question about the prediction of disease states or the assessment of the severity of the disease process. Subjects will need to be recruited to test the validity of BRSI.

An interesting observation from the data and the experimental setup was the fact that time frequency analysis was utilized to assess metal anxiety. However, without a properly designed protocol it will not be possible to verify these observations.

The difficulty with time frequency analysis was the ability to pull out the relevant information. The time-frequency distribution contained a lot of information and knowing how to extract it from the three dimensional graph was important. Looking at the three dimensional graph sometimes visually does not show anything. However, with the calculation of slope ,means and areas it was possible to extract the information .

The utilization of time-frequency analysis is vast. It may be used to study electromyographic changes during various conditions or to assess ANS damage. A future project may be the assessment of ANS damage in spinal cord injury patients. Measuring ANS response during voiding may indicate the severity of the damage to the urinary system. It is known how the autonomic nervous system operates during voiding. Comparison of the rate of change of the vagal tone or amplitude of healthy

subjects to spinal cord injured subjects may allow us categorize the severity of the injury.

There are may distributions that can perform time frequency analysis[1]. Each one has its own special properties. Depending on the nature of the signal some distributions may yield better results than others. Application of these other distributions to the fight or flight response files may be of interest. If there are other distributions that will yield better resolution of time and frequency and less noise, it might be advantageous to explore them.

BRSI may also be determined in the frequency domain[39]. This is another technique to evaluate the baroreceptor reflex. It might be interesting to compare the calculation of the time analysis technique to the frequency analysis technique. ECG and blood pressure are required for the calculation of BRSI using the frequency analysis technique. The data has already been acquired. What is required is the development of the computer software to extract the necessary information from the data.

## APPENDIX A

## PROCEDURE FOR CALCULATING BARORECEPTOR REFLEX SENSITIVITY INDEX

1. **R0371.FIN_PSLWSU(R0371)**
   pslwsu runs lws and creates an undecimated and decimated file.

2. **plot(R0371[,3])**
   Plot entire raw file containing blood pressure in colum 3 to choose interval containing phase IV of Valsalva.

3. **plot (R0371[6000:7000,3],col=2)**
   Plot approximate region of phase IV of Valsalva. (col=color)

4. **par(new=T)**
   Allows you to superimpose blood pressure and IBI.

5. **plot(R0371.fin$ibiu[6000:7000])**
   plot same region of undecimated IBI data.

6. From superimpose plot locate index on x-axis where blood pressure and IBI begin to increase together. (ie. blood pressure increasing while heart rate is decreasing.)

7. **plot(R0371[6500:6900,3],col=2)**
   plot specific region containing phase IV of Valsalva.

8. **R0371.bp_bp(R0371[6500:6900,3],R0371.fin$ibiu[6500:6900])**
   Calculates the systolic blood pressure peaks of phase IV of the Valsalva and its corresponding IBI values. A plot is generated with a least squared fit line with blood pressure on the x-axis and IBI on the y-axis.

9. **cor(R0371.bp$ppkv, R0371.bp$d)**
   Gives the correlation coefficient between systolic blood pressure peaks and corresponding IBI.

10. **R0371.bp$line**
    Gives slope and intercept of least squared fit line.

11. **BRSI= slope * 4.086*5**
    Converts slope index to ms/mmHg.

## APPENDIX B

### PROCEDURE FOR PERFORMING TIME-FREQUENCY ANALYSIS

1. From the .fin file obtain the ibi file and convert to .asc inorder to load to matlab. note: extension is not .asc but is still ASCII file.
   **write (jo62794.fin$ibi,file='j062794.ibi',ncol=1)**

2. Load into matlab
   **load c:\users\larry\j062794.ibi**

3. In order for the program to run the following changes in variable must be made. note: this is for graphical labeling
   **rawdata=j062794';**
   **top='j062794';**

4. Run program
   **sympar**

5. The following information will be useful in answering the questions the program asks.(parts a and b are for the lowpass filter used for detrending)
   a. Order of filter is usually **5**.
   b. Cutoff frequency is usually **.03**
   c. Sample rate of data is usually **20**
   d. Range for LF range
      i)Rest, 12& 18 bpm (.05-.15 Hz) for program enter index (1:4)
      ii) 8 bpm (.05-.1 Hz) for program enter index (1:4)
      iii) Exercise and Recovery (.05-.15 Hz) for program enter index (1:4)
   e Range for HF range
      i)Rest, 12 & 18 bpm (.15-.4 Hz) for program enter index (4:10)
      ii) 8 bpm (.1-.4 Hz) for program enter index (4:10)
      iii)Exercise & Recovery (.15-.8 Hz) for program enter index (4:20)
   note: In order to calculate index values divide the desired frequency by frequency resolution. Usually the frequency resolution is .0391 for an FFT of 512 and a sampling rate of 20. Index numbers are whole numbers so round.

6. After performing analysis on a file clear the matlab command window before starting another. This is to prevent writing over existing variables.
   **clear.**

# APPENDIX C

## COMPUTER PROGRAMS

BP was written in S-Plus to ascertain systolic blood pressure from Finapres blood pressure curve.

**BP**

```
function(x, y)
{
        sm <- smooth(x)
        ppk <- peaks(sm, span = 130)
        ppkp <- grep(T, ppk)
        ppkv <- sm[ppkp]
        d <- y[ppkp]
        plot(ppkv, d)
        line <- (lsfit(ppkv, d))
        abline(line)
        y <- list(d = d, ppkp = ppkp, ppkv = ppkv, line =
                line)
        y
}
```

The following programs were written in S-Plus to attain IIBI.

**IIBI**

```
function(x, sr = 1)
{
        y <- NA
        for(i in 1:length(x)) {
                y <- c(y, rep(x[i], round(x[i]/sr)))
        }
        y <- y[2:length(y)]
        y
}
```

**PSLWSU**

```
function(x)
{
        jks <- x[, 2]
        aa <- grep(T, diff(jks) > 1000)
```

```
        ljs <- lsbp(x, aa)
        ljs
    }
```

**LSPB**

```
    function(x, x.pk, nt = 8192, ns = 6, decimate = 10, tooruff
        = 0.8, f = 0.1, ld = 10, sd = 10)
    {
        mruff <- max(abs(ruff(diff(x.pk))))
        if(mruff >= tooruff)
            print(paste("ibi's may be too ruff", tooruff,
                sep = ""))
        x.ecg <- x[, 2]
        x.iu <- iibi(diff(x.pk))
        x.i <- x.iu[seq(1, len(x.iu), decimate)]
        x.sq <- sqdt(x.i, f = f, ld, sd)
        x.isp <- spect(x.i - x.sq, nt = nt, ns = ns)
        x.rpd <- x[seq(1, len(x[, 1]), 10), 1]
        x.rlw <- lowess(1:len(x.rpd), x.rpd, f = 0.3, iter
            = 2, delta = ceiling((length(x.rpd) * 0.3)/
            8))$y
        x.rsp <- spect(x.rpd - x.rlw, nt = nt, ns = ns)
        z <- list(pk = x.pk, ibi = x.i, ibiu = x.iu, sq =
            x.sq, rpd = x.rpd, rlw = x.rlw, isp = x.isp,
            rsp = x.rsp, ecg = x.ecg, )
        z
    }
```

The following program written in Matlab was utilized to perform time-frequency analysis on IIBI data.

**SYMPAR**

```
%Program calculates the Vagal tone and Sympo-vagal ratio.


order=input('Please enter the order of the lowpass filter. ');
freq=input('Please enter the cuttoff frequency for LPF. ');
sample=input('Please enter the sample rate of the data. ');
nfreq=freq/sample;
[poles,zeros]=butter(order,nfreq);
dtrend=filtfilt(poles,zeros,rawdata);
dtrendata=rawdata-dtrend;
[row,col]=size(dtrendata);
I=1:col;
```

```
%This  part is for testing Janse Kaiser Wigner calculatin algorithm with
% no window
fs=1000;
k=(col-512)/25;          %the number of spectra we compute
m=512;          % The size of the fft we will be computing.
T=1/fs;

w=ones(size(1:m));
x=hilbert(dtrendata);   % Forms the analytic funcion of x
L=m/2;
skip =25;       % Number of points we skip to get the next segment.
p=129;         %the number of freq vals we will be plotting
l=-(L-1):(L-1);
n=L;
for i=1:k
              %Here I think 0 lag is at the Lth point, hence the first
              % time location is at LT=128*.001 or .128 sec; hmmm.
       g=x(n+l).*conj(x(n-l));
       g(2*L)=0;
       y=w.*g; % Apply window to g or kernal.

       Y=2/m*abs(fft(y,512)); % evidently because it's analytic we only need 2/N
       Z(:,i)=Y(1:p)';
       n=n+skip;
end
%f=fs/(2*N)*(0:(N-1));
%plot(f,Y)
%Again it's strange. The fft has no mirror freqs because of analytic.
%But it looks like a perfectly good fft. I don't know what to say.
%It seems magic. Freq says 125 hz, amplitude says 1.
g=max(Z);
g=max(g);


Z1=Z;
clear Z;
Z=Z1(1:30,1:k);

LFC = input('Please enter the low frequency range in index numbers. ');
symvag=sum(Z(LFC,1:k));
HFC=input('Please enter the high frequency range in index numbers. ');
vagal=sum(Z(HFC,1:k));
symtopar=symvag./vagal;
```

```
%This is a file for determining the instantaneous frequency from the Wigner
%distribution.


n=128;          %The number of frequency values.
skip=25;
[r,c]=size(Z);  %Determines the size of the matrix created by wgjka4.m.
for i=1:c;      %Repeation based on number of columns.
W=Z(:,i);       %W is assigned the values of the column.
Y=(1:r)';       %Y represents the frequencies.
M=W.*Y;
S=sum(M);
F=sum(W);       %Sum of the Wigner Distribution values.
E(i)=S/F;
end


% Plotting commands
subplot(3,1,1);
plot(I,rawdata,'r',I,dtrend,'g');
title(top);
xlabel('time')
ylabel('amplitude')

subplot(3,1,2);
plot(dtrendata);
title('IBI detrended');
xlabel('time');
ylabel('amplitude');

subplot(3,1,3);
plot(E);
xlabel('time');
ylabel('frequency');
title('Instantaneous frequency');

print

subplot(1,1,1);

subplot(2,1,1);
mesh(Z);
xlabel('time');
ylabel('frequency');
title(top);
```

```
subplot(2,1,2);
contour(Z);
xlabel('time');
ylabel('frequency');
title('Contour plot of WD');

print

subplot(3,1,1);
plot(symvag);
gtext(top);
title(' Mixture of Sympathetic and Parasympathetic');
xlabel('time');
ylabel('amplitude');

subplot(3,1,2);
plot(vagal);
title('Parasympathetic range');
xlabel('time');
ylabel('amplitude');

subplot(3,1,3);
plot(symtopar);
title('Ratio of  Low Frequency to High Frequency')
xlabel('time');
ylabel('amplitude');

print
```

Programs used to generated sine and chirp.

**Sine**

```
n=1:100;
x=sin(2*pi*10*n);
```

**Chirp**

```
n=1:100;
l=1:50;
x=sin(2*pi*l .*n)
```

## REFERENCES


1. Classen, T.A.C.M., and W.F.G Mecklenbrauker. "The Wigner Distribution-a Tool for Time-Frequency Signal Analysis," Philips J. Res. 35, (1980) Part I, 217-250; Part II, 276-300; Part III, 372-389.

2. Amin, M., Cohen, L. and W.J. Williams. "Methods and Applications for Time-Frequency Analysis" Conference Notes, University of Michigan (1993).

3. Hlawatsch, F., and G.F. Boudreaux-Bartels. "Linear and Quadratic Time-Frequency Signal Representations" IEEE SP Magazine (April 1992) : 21-67.

4. Ziemer, R.E., Tranter, W.H. and D.R. Fannin. *Signals and Systems: Continuous and Discrete*, 2nd edition, New York, Macmillan Publishing Company (1989).

5. Abeysekera, R.M.S.S. and B. Boashash. "Time-Frequency Domain Features of ECG Signals: Their Applications in P-wave Detection using the Cross Wigner-Ville Distribution." IEEE Int. Conf. Acoust., Speech, Sig. Proc. Glasgow, Scotland.(1989).

6. Novak, P. and V. Novak."Time/Frequency Mapping of the Heart Rate, Blood Pressure and Respiratory Signals." Medical & Biological Engineering & Computing.(March 1993) : 103-110.

7. Yen, N. "Time and Frequeny Representation of Acoustic Signals by Means of the Wigner Distribution function: Implementation and Interpretation," J. Acoust. Soc. Am. 81(6), (June 1987) :1841-1850.

8. Curtis, H. and N.S. Barnes. *Biology* 5th edition., New York, Worth Publishers, INC., (1989); 841-857.

9. Vander, A.J., Sherman, J.H. and D.S. Luciano. *Human Physiology*, 5th edition.,New York, McGraw-Hill Publishing Company (1990).

10. Hockman, C.H. *Essentials of Autonomic Function*, IL, Springfield (1987).

11. Ganong, W.F. *Review of Medical Physiology*, New York, Applicon & Lange (1993).

12. Bannister, S.R. and C.J. Mathias. *Autonomic Failure : A Textbook of Clinical Disorders of the Autonomic Nervous System*, 3rd edition. New York, Oxford University Press, (1992) : 312-333.

13. Palmero H.A.,Caeiro T.F. Iosa D.J. and J. Bas. "Baroreceptor Reflex Sensitivity Index Derived from Phase 4 of the Valsalva Maneuver." Hypertension 3 Suppl 2 (1981):134-137.

14. Nishimura, R.A. and A.J. Tajik."Cardiovascular Clinics: The Valsalva Maneuver and Response Revisited." Mayo Clin Proc.,(1986) 61:211-217.

15. Elisberg, EI." Heart Rate Response to the Valsalva Maneuver as a Test of Circulatory Integrity." JAMA (1973); 186:120.

16. Hamilton, W.G., Woodburry, R.A. and H.T. Harper Jr." Physiologic Relationships Between Intrathoracic , Intraspinal and Arterial Pressure." JAMA (1986); 107:853-8.

17. Wang, X., Reisman, S.S., Tapp W.N. and B.H. Natelson. "Spectrum Analysis of Heart Rate Variability." Proceedings of the Eleventh Annual Meeting of the IEEE Engineering in Medicine and Biology, (1990).

18. Shin, S., Tapp,W.N., Reisman,S.S. and B.H. Natelson. "Assessment of Autonomic Regulation of Heart Rate Variability by the Method of Complex Demodulation," IEEE Transactions on Biomedical Engineering, Vol 36 No. 2 (Feb 1989) : 274:282

19. Akselrod, S., Gordon, D., Madwed, J.B., Snidman, N.C., Shannon, D.C. and R.J. Cohen. "Hemodynamic Regulation: Investigation by Spectral Analysis," Am. J. Physiol. 249, (1985): H867-75.

20. Pomeranz,B., Macaulay,R.J.B., Caudill, M.A., Kutz, I., Adam, D., Gordon. D., Kilborn, K.M., Barger, A.C., Shannon, D.C., Cohen, R.J. and H. Benson."Assessment of Autonomic Function in Humans by Heart Rate Spectral Analysis,"Am. J. Physiol. 248, (1985):H151-3.

21. Pagani, M., Lombardi, F., Guzzetti, S., Rimoldi, O., Furlan, R., Pizzinelli, P.,Sandrone, G., Malfatto, G.,Del' Orto, S., Piccaluga, E., Turiel, M., Baselli, G.,Cerutti, S. and A. Malliani. "Power Spectral Analysis of Heart Rate and Arterial Pressure Variabilities as a Maker of Sympatho-vagal Interaction in Man and Conscious Dog. Circulation Res., 59, (1986): 178-93.

22. Furlan, R., Guzzetti, S., Crivellaro, W., Dassi, S., Tinelli, M., Baselli, G., Cerutti, S., Lombardi, F., Pagani, M. and A. Malliani. "Continuous 24-hour assessment of the neural regulation of systemic arterial pressure and RR variabilities in ambulant subjects," Circulation 81, (1990) : 537-47.

23. Chess, G.F., Tam, R.M.K and F.R. Calresu. "Influences of Cardiac Neural Inputs on Rhythmic Variations of Heart Period in the Cat," Amer. J. Physiol., vol. 228, (1975) :775-780.

24. Luczak, H. and W. Laurig. "An Analysis of Heart Rate Variability," Ergonomics,vol. 16, no. 1,(1973): 85-97.

25. *2300 Finapress Blood Pressure Monitor* ,Operation Manual, Louisville,Ohmeda CO.1991.

26. Wesseling, K.H., Settles, J.J. and B. deWit. *The Measurement of Continuous Finger Arterial Blood Pressure Non-invasively in Stationary Subjects.* In: *Biological and Psychological Factores in Cardiovascular Disease.* Schmidt, T.H.; Dembroski, T.M.,and G. Blumchen (eds.) , (1986):355-375.

27. LaRovere,M.T., Speechia G., Mortara, A. and P.J. Schwartz P.J. "Baroreflex Sensitivity , Clinical Correlates, and Cardiovascular Mortality Among Patients with a First Time Myocardial Infarction." Circulation, 78(4), (1988):816-824.

28. Goldstein, D.S., Horwitz D. and H.R. Keiser. "Comparison of Techniques for Measuring Baroreflex Sensitivity in Man." Circulation (1982); 66(2):432-439.

29. Knaflitz, M. and B. Gabriella. "Computer Analysis of the Myoelectric Signal." IEEE Micro. (1991), 10:12-15,48-58.

30. Basmajian, J.V. and C.J. DeLuca. *Muscles Alive.* John Butler. 5th edition Baltimore: Williams & Wilkins (1985).

31. Marieb, E.N. "Muscles and Muscle Tissue." *Human Anatomy and Physiology.* 2nd edition. California, The Benjamin/Cummings Publishing Company,Inc. (1992):246-269.

32. Davies, Michelle R. "Time Frequency Analysis of Electromyogram During Mucle Fatigue", NJIT thesis, January 1994.

33. DeLuca, C.J., Sabbahi, M.A., Stulen,F.B. and G. Bilotto. "Some Properties of the Median Frequency of the Myoelectric Signal during Localized Muscular Fatigue." Proceeding of the 5th International Symposium of the Biochemistry of Exercise. Human Kinetic Publishers, Chicago.(1983): 175-186.

34. Smith, M.L., Hudson, D.L., Graitzer, H.M. and P.B. Raven. "Exercise Training Bradycardia: the Role of Autonomic Balance." Med Sci Sports Exer. 21(1) (1989):40-44.

35. Kunsten, R., Kunsten S.F., Curb J.D., Reed D.M., Kautz J.A. and K. Yano. "Predicitive Value of Resting Electrocardiogram for 12-year Incidence of Stroke in the Honolulu Heart Program." Stroke (1988); 19(5):555-9.

36. McLeod, J.G. and R.R.Tuck. "Disorders of the Autonomic Nervous System. I. Pathophysiology and Clinical Features," Ann. Neurol.,21, 419, (1987).

37. Roth, E.J., Mueller, K. and D. Green. "Stroke Rehabilitation: Cardiovascular Response to Physical Therapy." J. NeuroRehabil 1992; 2(2): 7-15.

38. Ferrer, M.T., Kennedy, W.R. and F. Sahinen. "Baroreflexes in Patients with Diabetes Mellitus." Neurology. 41(1991):1462-1466.

39. Hindrik, W.J., Lambertus, J.M.,Ruddel,M.H., Langewitz,W.A., Johannes and Gusbertus Mulder. "Assessment of Baroreceptor Reflex Sensitivity by Means of Spectral Analysis." Hypertension vol 10, No 5, (November 1987): 538:543.